Neurobiology of Disease 161 (2021) 105545

Contents lists available at ScienceDirect

Neurobiology of Disease

journal homepage: www.elsevier.com/locate/ynbdi

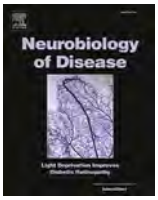

Regulation of NRG-1-ErbB4 signaling and neuroprotection by exogenous neuregulin-1 in a mouse model of epilepsy

Allison R. Peterson, Terese A. Garcia, Byron D. Ford, Devin K. Binder *

Division of Biomedical Sciences, School of Medicine, Center for Glial-Neuronal Interactions, University of California, Riverside, CA, USA

ARTICLE INFO

Keywords:
Neuregulin-1
Epilepsy
ErbB4
Neuroprotection
EAAC1
Glutamate synthetase
GFAP

ABSTRACT

Temporal lobe epilepsy (TLE) is the most common form of focal epilepsy. Dysregulation of glutamate transporters has been a common finding across animal models of epilepsy and in patients with TLE. In this study, we investigate NRG-1/ErbB4 signaling in epileptogenesis and the neuroprotective effects of NRG-1 treatment in a mouse model of temporal lobe epilepsy. Using immunohistochemistry, we report the first evidence for NRG-1/ErbB4-dependent selective upregulation of glutamate transporter EAAC1 and bihemispheric neuroprotection by exogeneous NRG-1 in the intrahippocampal kainic acid (IHKA) model of TLE. Our findings provide evidence that dysregulation of glutamate transporter EAAC1 contributes to the development of epilepsy and can be therapeutically targeted to reduce neuronal death following IHKA-induced status epilepticus (SE).

1. Introduction

Epilepsy is a common neurological disorder characterized by unprovoked seizures affecting more than 70 million people worldwide (Fisher et al., 2014; Singh and Trevick, 2016). Temporal lobe epilepsy (TLE) is the most common form of epilepsy with focal seizures. Approximately 30% of patients with TLE suffer from refractory epilepsy whose seizures cannot be controlled with currently available antiepileptic drugs (AEDs) (Dalic and Cook, 2016). Current AEDs primarily target neurons directly by attenuating glutamatergic neurotransmission or enhancing GABAergic neurotransmission. The most common AEDs work by targeting voltage- and ligand-gated ion channels including voltage-gated Na^+ channels, voltage-gated Ca^{2+} channels, voltage-gated K^+ channels, the GABA γ-aminobutyric acid (GABA) receptor channel complex, and ionotropic glutamatergic receptors (Beck and Yaari, 2012). Although several newer generation AEDs have appeared, multiple studies have shown that the effectiveness of these AEDs to control seizures is not stronger than that of old generation AEDs (Lee, 2014). Inhibition of excitatory neurotransmission, a frequent target of many AEDs, can have deleterious cognitive side effects that have been shown to lead to drug discontinuation therefore there is a need for alternative therapeutics to treat patients with epilepsy (Brodie et al., 2016).

Chronically elevated glutamate is a common pathological feature observed in preclinical models and patients with refractory TLE (Eid et al., 2004; Cavus et al., 2016). Na^+-dependent glutamate transporters are responsible for the majority of glutamate uptake in the central nervous system (CNS). Extracellular glutamate homeostasis is essential for efficient and localized synaptic neurotransmission (Mahmoud et al., 2019). Excitatory amino acid transporter 1 (EAAT1)/glutamate aspartate transporter (GLAST) and excitatory ammino acid transporter 2 (EAAT2)/glutamate transporter-1 (GLT-1) are primarily found on astrocytes while excitatory amino acid transporter 3 (EAAT3)/excitatory amino acid carrier 1 (EAAC1) is primarily neuronal (Danbolt, 2001). Astrocytic EAAT2 protects against fatal epilepsy and performs critical functions in the CNS (Petr et al., 2015). Multiple studies have shown that GLT-1 is downregulated in animal models and patients with TLE while upregulation of GLT-1 in animal models reduces seizures and can improve behavioral outcome (Peterson and Binder, 2019; Peterson et al., 2021; Ramandi et al., 2021). The neuronal glutamate transporter EAAC1, although not a major player in glutamate homeostasis, is a major route of neuronal cysteine uptake which is important for the synthesis of glutathione (GSH), an antioxidant important in regulating redox homeostasis and protection against stress induced neurotoxicity. Astrocytic glutamine synthetase is responsible for the rapid conversion of intracellular glutamate to glutamine following glutamate uptake by astrocytic glutamate transporters and is a prerequisite for efficient glutamate clearance from the extracellular space (Eid et al., 2013). Loss of glutamine synthetase has also been observed in patients with TLE which could have an impact on glutamate transporter clearance (Eid et al., 2004). EAAC1 and GSH have also been shown to be dysregulated

* Corresponding author at: Division of Biomedical Sciences, University of California, Riverside, 1247 Webber Hall, Riverside, CA 92521, USA.
E-mail address: dbinder@ucr.edu (D.K. Binder).

https://doi.org/10.1016/j.nbd.2021.105545
Received 15 September 2021; Received in revised form 28 October 2021; Accepted 2 November 2021
Available online 3 November 2021

in animal models and patients with epilepsy (Crino et al., 2002; Proper et al., 2002; Shin et al., 2008).

Neuregulin-1 (NRG-1), a growth factor with various functions in the CNS, plays an important role in development, neuroplasticity and repair (Cespedes et al., 2018). NRG-1 shares an epidermal growth factor (EGF)-like domain with the tyrosine kinase receptor, epidermal growth factor receptor 4 (ErbB4). Previous studies have shown that NRG-1/ErbB4 signaling is activated following brain insult and protects neurons from glutamate-induced death (Cannella et al., 1999; Erlich et al., 2000; Parker et al., 2002; Deng et al., 2019; Noll et al., 2019). NRG-1 signaling through ErbB4 has also been shown to modulate the Na^+-dependent glutamate transporter, EAAC1, and increase glutamate uptake in neurons through upregulation of EAAC1 (Yu et al., 2015). In this study, we examine the regulation of endogenous NRG-1/ErbB4 signaling and EAAC1 modulation in epilepsy and determine the therapeutic effects of exogenous NRG-1 (25 μg/kg/day) treatment at early phases of epileptogenesis.

2. Methods

2.1. Animals

8–10-week-old Charles River CD1 male mice were housed under a 12-hour light and 12-hour dark cycle with *ad libitum* access to food and water. All experiments performed were approved by the University of California, Riverside Institutional Animal Care and Use Committee (IACUC) and were conducted in accordance with the National Institutes of Health (NIH) guidelines. A total of 28 mice were used for this study.

2.2. Intrahippocampal kainic acid administration

Intrahippocampal kainic acid (IHKA) injections were used to induce epileptogenesis as previously described (Lee et al., 2012; Hubbard et al., 2016; Peterson and Binder, 2019). Mice were anesthetized with a solution of ketamine (80 mg/kg)/xylazine (10 mg/kg) and positioned in a stereotaxic frame. The skull was exposed, bregma was located, and a craniotomy was performed 1.8 mm posterior and 1.6 mm lateral to bregma. Mice were injected with 64 nL of 20 mM kainic acid (Tocris) or 64 nL of 0.9% saline using a microinjector (Nanoject II, Drummond Scientific) into the *CA1* region of the dorsal hippocampus (1.9 mm dorsoventral coordinate). Mice were given buprenorphine to minimize discomfort. Following surgery, all mice injected with kainic acid were video recorded for at least 8 h. All mice included in the study experienced status epilepticus (SE), defined by Racine scale stage 3–5 seizures (Racine, 1972) for at least 3 h.

2.3. NRG-1 treatment

Mice were given either NRG-1 (25 μg/kg/day; R&D Systems Part # 396-HB-050) or vehicle (0.1% Bovine Serum Albumin) intraperitoneal daily for 7 days following IHKA injection as previously described (Liu et al., 2018). The first dose of NRG-1 or vehicle was administered immediately after IHKA injection followed by daily injections. No treatment was given on the day of euthanasia (day 7 post-IHKA induced status epilepticus) (Fig. 1).

2.4. Immunohistochemistry

Mice were euthanized 7 days post-IHKA with Fatal Plus (Western Medical Supply) then perfused with ice-cold phosphate buffered saline (PBS) followed by 4% paraformaldehyde (PFA). Brains were harvested and fixed in 4% PFA for two hours at room temperature (RT). Harvested brains were then transferred and stored in 30% sucrose at 4 °C until use. Prior to sectioning, harvested brains were flash frozen with isopentane. Frozen brains were sealed in optimum cutting temperature (O.C.T.) formulation at 20 °C and sliced into 50 μm sections using a cryostat

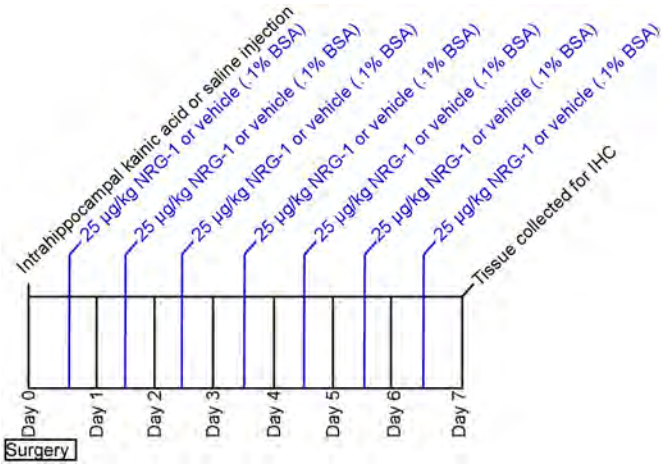

Fig. 1. Overview of experimental design. Mice were unilaterally injected with kainic acid (20 mM) or saline into the dorsal hippocampus. A subset of mice injected with kainic acid were given 25 μg/kg NRG-1 or vehicle (0.1% BSA) intraperitoneal daily for 7 days. Tissue was collected at 7 days post-IHKA induced SE for immunohistochemistry.

(Leica CM 1950). Sections were stored in 0.01% sodium azide PBS at 4 °C. Slices were collected from each animal (Saline n = 6 animals; IHKA n = 6; IHKA + Vehicle n = 5; IHKA + Treated n = 6). For each animal, per stain, 2 sections were processed for immunohistochemistry, 1 ventral and 1 dorsal to the injection site. For immunohistochemistry, sections were washed with PBS, permeabilized with 0.5% Triton-X-100 for 10 min at RT, quenched with 3% H_2O_2, and blocked for 1 h at RT with 10% bovine serum albumin (BSA)/0.5% Triton-X-100. Sections were then incubated overnight at 4 °C in 10% BSA/0.5% Triton-X-100 with primary antibodies to NRG1 type III (1:200, Millipore MAB360), ErbB4 phospho Y1284 (1:200, ab61059), EAAT3 [EPR6774(B)] (1:200, Abcam ab124802), GFAP (1:200, MAB360), NeuN (1:200, EMD Millipore MAB377), NeuN (1:200, EMD Millipore ABN78), Parvalbumin (1:1000, Sigma-Aldrich P3088), Iba1 (1:500, Abcam ab178846), Glutamine synthetase (1:200, EMD Millipore G2781), EAAT1 (1:200, Abcam Ab416), and GLT-1 (1:400, cGLT1a antibody generously provided by Dr. Jeff Rothstein). Sections were washed with PBS and incubated with HRP-conjugated secondary antibodies (HRP Goat Anti-Rabbit; 1:200, BIOTUM Tyramide Amplification Kit 33,001) 1 h RT. Sections were then incubated with 488A Tyramide (1:500) in working amplification buffer 10 min RT. Then sections were washed and incubated with Alexa 594 (Molecular Probes/Invitrogen) for 1.5 h for visualization and mounted in ProLong Gold Antifade with DAPI.

2.5. Imaging and quantification

Hippocampal images were captured at 5×, 20×, 40×, and 63× magnification using a fluorescence microscope (Leica DM6 B) under identical settings for each channel. Quantification was performed using ImageJ software. Individual boxes identifying individual layers region of interest (ROIs) were drawn on the DAPI channel at the center of each layer of the hippocampus: *stratum* (*s.*) *oriens*, *s. pyramidale* of *CA1*, *s. radiatum*, *s. lacunosum moleculare* (SLM), molecular layer, upper blade of the dentate gyrus, hilus, lower blade of the dentate gyrus, *s. lucidum*, and *s. pyramidale* of *CA3* as previously described (Peterson and Binder, 2019). For NeuN immunoreactivity quantification, mean gray value was calculated across the entire image for each region of interest: *s. pyramidale* of *CA1*, *s. pyramidale* of *CA3*, and the dentate gyrus as previously described (Peterson et al., 2021). For parvalbumin immunoreactivity quantification, a region of interest was drawn around the hippocampus and mean gray value was calculated across the entire region.

2.6. Statistical analysis

Statistical analysis was performed using Prism 8 software (GraphPad Software, La Jolla, CA. Datasets were analyzed using an unpaired two-tailed *t*-test with a 95% confidence interval (CI). For datasets for NRG-1/ErbB4 and EAAC1 expression comparing NRG-1 treated animals *vs.* vehicle an unpaired one-tailed t-test with a 95% confidence interval was used for analysis. All error bars are presented as the mean ± standard error of the mean (SEM). Difference between groups was considered statistically significant by a P-value ≤0.05 and was denoted with one asterisk (*).

3. Results

3.1. Endogenous NRG-1/ErbB4 signaling is increased post-IHKA induced SE

Hippocampal NRG-1 and phospho-ErbB4 immunoreactivity was assessed at 7 days post-IHKA induced SE compared to saline-injected control mice. Quantification of individual hippocampal layers was performed for both hippocampi ipsilateral (Fig. 2, Fig. 4) and contralateral (Fig. 3, Fig. 5) to injection at 7 days post-IHKA induced SE. NRG-1/ErbB4 activity was elevated in the epileptic hippocampus post-IHKA induced SE. Two-tailed *t*-tests on NRG-1 immunoreactivity of individual hippocampal layers in the ipsilateral hippocampus at 7 days post-IHKA induced SE revealed a main effect of treatment (Fig. 2). NRG-1 immunoreactivity was significantly increased in *stratum (s.) oriens* (t(df) = 2.646 (19), p = 0.0159; mean ± SEM: Saline = 22.07 ± 2.918; IHKA = 33.82 ± 3.300), *s. pyramidale* of *CA1* (t(df) = 2.442 (19), p = 0.0246; mean ± SEM: Saline = 25.62 ± 3.363; IHKA = 39.43 ± 4.436), *s. radiatum* (t(df) = 2.533 (19), p = 0.0203; mean ± SEM: Saline = 19.42 ± 2.169; IHKA = 29.62 ± 3.291), and *s. lacunosum moleculare* (t(df) = 2.288 (19), p = 0.0338; mean ± SEM: Saline = 22.70 ± 2.685; IHKA = 32.82 ± 3.432) in the ipsilateral hippocampus 7 days post-IHKA induced SE compared to saline-injected control mice (Fig. 2). Two-tailed *t*-tests on NRG-1 immunoreactivity of individual hippocampal layers in the contralateral hippocampus at 7 days post-IHKA revealed no effect of treatment (p > 0.05) (Fig. 3).

Phospho-ErbB4 immunoreactivity was increased in *CA1* in the ipsilateral hippocampus 7 days post-IHKA induced SE. A two-tailed *t*-test on phospho-ErbB4 immunoreactivity of *s. pyramidale* of *CA1* in the ipsilateral hippocampus at 7 days post-IHKA revealed phospho-ErbB4 immunoreactivity was significantly increased in *s. pyramidale* of *CA1* (t(df) = 3.186 (16), p = 0.0057; mean ± SEM: Saline = 11.11 ± 1.261; IHKA = 19.32 ± 2.062) in the ipsilateral hippocampus 7 days post-IHKA induced SE compared to saline-injected control mice (Fig. 4). Two-tailed *t*-tests on phospho-ErbB4 immunoreactivity of individual hippocampal layers in the contralateral hippocampus at 7 days post-IHKA revealed no effect of treatment (p > 0.05) (Fig. 5).

3.2. NRG-1/ErbB4 signaling is increased in mice treated with exogenous NRG-1 post-IHKA induced SE

Hippocampal NRG-1 and phospho-ErbB4 immunoreactivity was assessed in the hippocampus of NRG-1 (25 μg/kg/day) treated *vs.* vehicle (0.1% Bovine Serum Albumin) treated mice at 7 days post-IHKA induced SE. Quantification of individual hippocampal layers was performed for both hippocampi ipsilateral (Fig. 6, Fig. 8) and contralateral (Fig. 7, Fig. 9) to injection at 7 days post-IHKA induced SE. NRG-1/ErbB4 activity was elevated in NRG-1 treated mice in both hippocampi ipsilateral and contralateral to injection 7 days post-IHKA induced SE. One-tailed t-tests on NRG-1 immunoreactivity of individual hippocampal layers in the ipsilateral hippocampus at 7 days post-IHKA revealed a main effect of NRG-1 treatment (Fig. 6). NRG-1 immunoreactivity was significantly increased in the molecular layer (t(df) = 2.396 (18), p = 0.0138; mean ± SEM: Vehicle = 21.31 ± 0.9605; NRG-1 Treated = 32.09 ± 3.976), upper granule cell layer (GCL) (t(df) = 2.737 (18), p = 0.0068; mean ± SEM: Vehicle = 17.57 ± 0.7151; NRG-1 Treated = 31.02 ± 4.384), hilus (t(df) = 2.012 (18), p = 0.0297; mean ± SEM: Saline = 21.41 ± 1.350; IHKA = 32.56 ± 4.869), lower GCL (t(df) = 2.920(18), p = 0.0046; mean ± SEM: Vehicle = 15.56 ± 0.8068; NRG-1 Treated = 28.25 ± 3.856), *s. pyramidale* of *CA3* (t(df) = 2.503 (18), p = 0.0111; mean ± SEM: Vehicle = 25.39 ± 1.347; NRG-1 Treated = 38.80 ± 4.695) and *s. lucidum* (t(df) = 2.503 (18), p = 0.0111; mean ± SEM: Vehicle = 25.39 ± 1.347; NRG-1 Treated = 38.80 ± 4.695) in NRG-1 treated mice in the ipsilateral hippocampus 7 days post-IHKA induced SE compared to vehicle (Fig. 6).

One-tailed *t*-tests on NRG-1 immunoreactivity of individual hippocampal layers in the contralateral hippocampus at 7 days post-IHKA revealed a main effect of NRG-1 treatment in all layers (Fig. 7). NRG-1 immunoreactivity was significantly increased in *s. oriens* (t(df) = 2.801 (19), p = 0.0057; mean ± SEM: Vehicle = 20.21 ± 1.286; NRG-1 Treated = 30.08 ± 3.141), *s. pyramidale* of *CA1* (t(df) = 2.943 (19), p = 0.0042; mean ± SEM: Vehicle = 20.62 ± 1.643; NRG-1 Treated = 31.57 ± 3.210), *s. radiatum* (t(df) = 2.563 (19), p = 0.0095; mean ± SEM: Vehicle = 20.12 ± 1.407; NRG-1 Treated = 26.09 ± 1.811), *s. lacunosum moleculare* (t(df) = 3.198 (19), p = 0.0024; mean ± SEM: Vehicle = 20.70 ± 0.5479; NRG-1 Treated = 28.49 ± 2.260), the molecular layer (t(df) = 3.466 (19), p = 0.0013; mean ± SEM: Vehicle = 17.86 ± 0.5362; NRG-1 Treated = 28.74 ± 2.944), upper GCL (t(df) = 3.548 (19), p = 0.0011; mean ± SEM: Vehicle = 15.38 ± 0.6232; NRG-1 Treated = 26.56 ± 2.944), hilus (t(df) = 3.541 (19), p = 0.0011; mean ± SEM: Vehicle = 15.12 ± 0.5380; NRG-1 Treated = 26.53 ± 3.026), lower GCL (t(df) = 4.045 (19), p = 0.0003; mean ± SEM: Vehicle = 14.42 ± 0.6256; NRG-1 Treated = 26.55 ± 2.794), *s. pyramidale* of *CA3* (t(df) = 3.359 (19), p = 0.0016; mean ± SEM: Vehicle = 20.43 ± 0.6787; NRG-1 Treated = 33.06 ± 3.524), and *s. lucidum* (t(df) = 3.303 (19), p = 0.0019; mean ± SEM: Vehicle = 14.71 ± 0.7481; NRG-1 Treated = 23.78 ± 2.522) in NRG-1 treated mice in the contralateral hippocampus 7 days post-IHKA induced SE compared to vehicle (Fig. 7).

Phospho-ErbB4 immunoreactivity was increased in both hippocampi ipsilateral and contralateral to injection in NRG-1-treated mice *vs.* vehicle (Fig. 8, Fig. 9). One-tailed *t*-tests on phospho-ErbB4 immunoreactivity of individual hippocampal layers in the ipsilateral hippocampus at 7 days post-IHKA revealed a main effect of NRG-1 treatment in all layers (Fig. 8). Phospho-ErbB4 immunoreactivity was significantly increased in *s. oriens* (t(df) = 2.610 (15), p = 0.0098; mean ± SEM: Vehicle = 15.95 ± 1.196; NRG-1 Treated = 23.79 ± 2.615), *s. pyramidale* of *CA1* (t(df) = 3.556 (15), p = 0.0014; mean ± SEM: Vehicle = 18.91 ± 1.181; NRG-1 Treated = 30.26 ± 2.812), *s. radiatum* (t(df) = 2.895 (15), p = 0.0055; mean ± SEM: Vehicle = 14.46 ± 0.7099; NRG-1 Treated = 21.99 ± 2.360), *s. lacunosum moleculare* (t(df) = 2.608 (15), p = 0.0099; mean ± SEM: Vehicle = 14.85 ± 0.8222; NRG-1 Treated = 20.29 ± 1.818), the molecular layer (t(df) = 3.260 (15), p = 0.0026; mean ± SEM: Vehicle = 9.805 ± 0.3653; NRG-1 Treated = 19.44 ± 2.759), upper GCL (t(df) = 2.952 (15), p = 0.0049; mean ± SEM: Vehicle = 9.049 ± 0.3012; NRG-1 Treated = 17.37 ± 2.635), hilus (t(df) = 2.591 (15), p = 0.0102; mean ± SEM: Vehicle = 10.89 ± 0.5448; NRG-1 Treated = 20.45 ± 3.432), lower GCL (t(df) = 3.170 (15), p = 0.0032; mean ± SEM: Vehicle = 7.340 ± 0.3366; NRG-1 Treated = 16.53 ± 2.708), *s. pyramidale* of *CA3* (t(df) = 2.755 (15), p = 0.0074; mean ± SEM: Vehicle = 10.37 ± 0.7949; NRG-1 Treated = 20.16 ± 3.263), and *s. lucidum* (t(df) = 3.131 (15), p = 0.0034; mean ± SEM: Vehicle = 9.286 ± 1.122; NRG-1 Treated = 19.26 ± 2.824) in NRG-1 treated mice in the ipsilateral hippocampus 7 days post-IHKA induced SE compared to vehicle (Fig. 8).

One-tailed *t*-tests on phospho-ErbB4 immunoreactivity of individual hippocampal layers in the contralateral hippocampus 7 days post-IHKA revealed a main effect of NRG-1 treatment in all layers (Fig. 9). Phospho-ErbB4 immunoreactivity was significantly increased in *s. oriens* (t(df) = 3.377 (17), p = 0.0018; mean ± SEM: Vehicle = 10.14 ± 0.8214; NRG-1 Treated = 18.56 ± 2.026), *s. pyramidale* of *CA1* (t(df) = 3.001 (17), p =

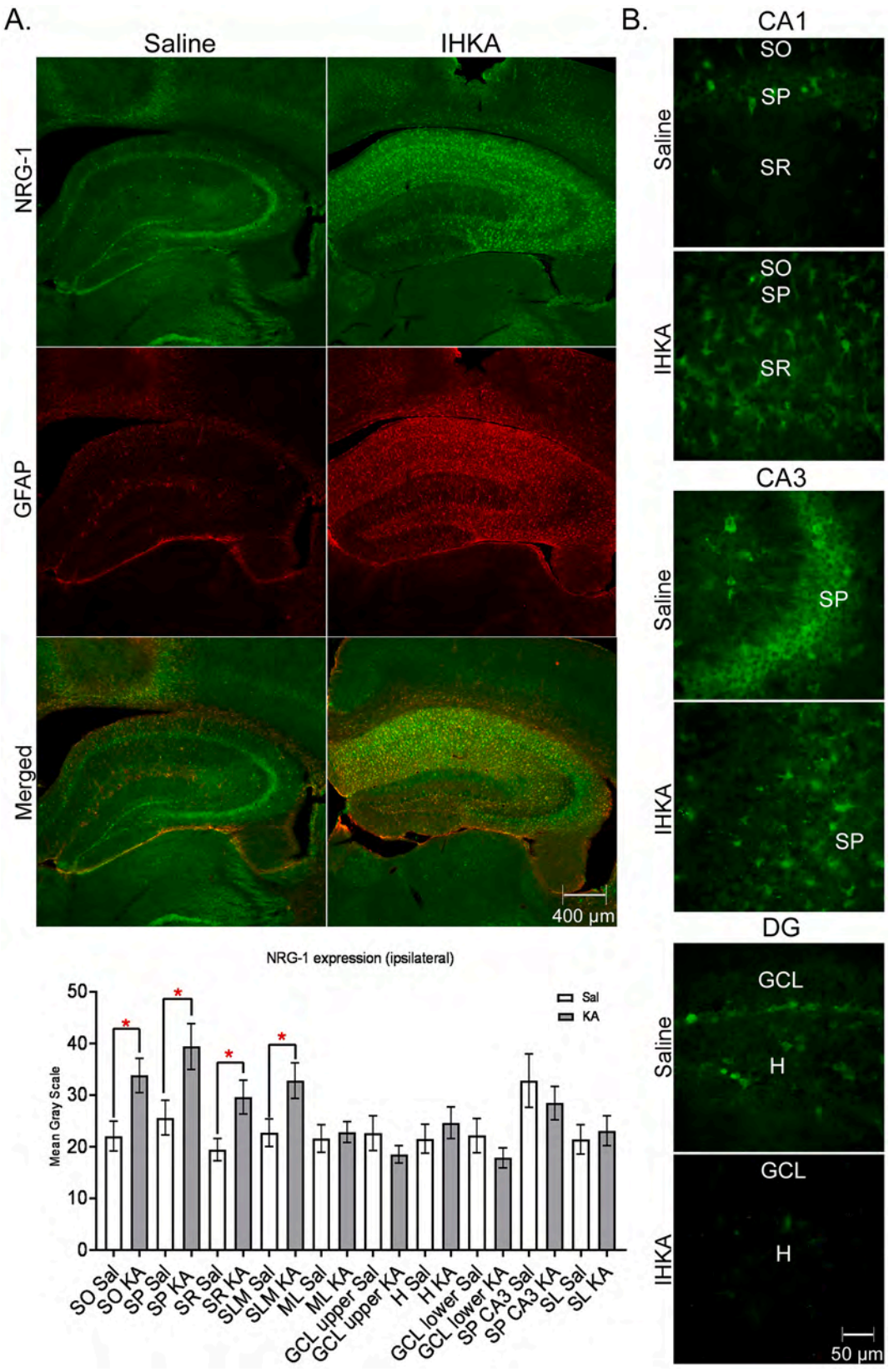

Fig. 2. Neuregulin-1 (NRG-1) expression is increased in the ipsilateral hippocampus 7 days post-IHKA induced SE. A. NRG-1 (green) and GFAP (red) expression in the ipsilateral hippocampus 7 days post-IHKA induced SE *vs.* saline-injected control mice (5×). NRG-1 mean gray scale quantitation of individual cell layers. B. NRG-1 expression in CA1, CA3 and DG at 7 days post-IHKA induced SE (40×). SO = *Stratum Oriens*; SP = Stratum *Pyramidale*; SR = *Stratum Radiatum*; SLM = *Stratum Lacunosum Moleculare*; GCL = Granule Cell Layer; H = Hilus SL = *Stratum Lucidum*. Saline group; N = 10 sections (5 mice). IHKA group; N = 11 sections (6 mice). (For interpretation of the references to colour in this figure legend, the reader is referred to the web version of this article.)

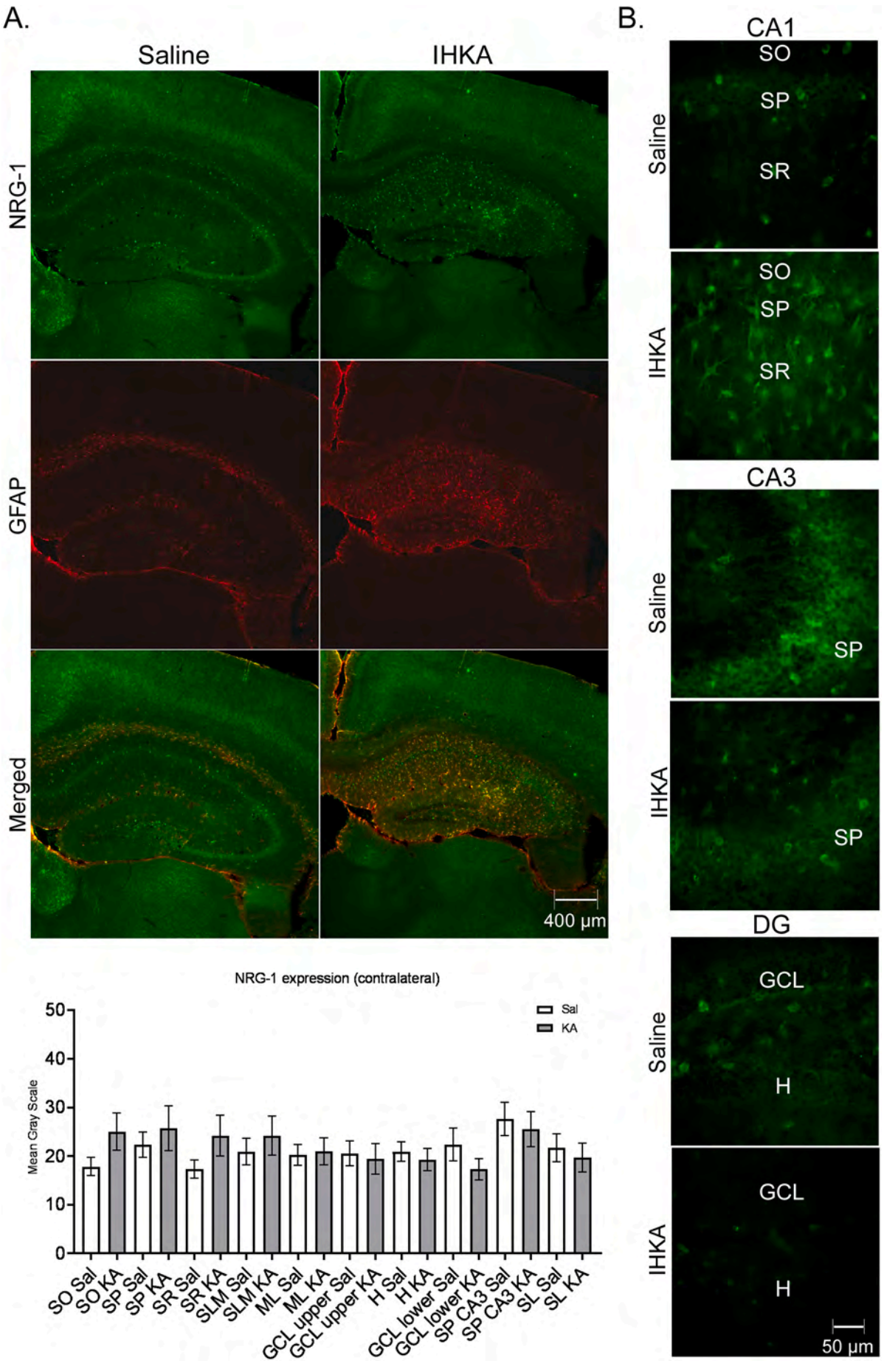

(caption on next page)

Fig. 3. Neuregulin-1 (NRG-1) expression in the contralateral hippocampus 7 days post-IHKA induced SE. A. NRG-1 (green) and GFAP (red) expression in the contralateral hippocampus 7 days post-IHKA induced SE *vs.* saline-injected control mice (5×). NRG-1 mean gray scale quantitation of individual cell layers. B. NRG-1 expression in CA1, CA3 and DG at 7 days post-IHKA induced SE (40×). SO = *Stratum Oriens*; SP = *Stratum Pyramidale*; SR = *Stratum Radiatum*; SLM = *Stratum Lacunosum Moleculare*; GCL = Granule Cell Layer; H = Hilus SL = *Stratum Lucidum*. Saline group; N = 11 sections (6 mice). IHKA group; N = 12 sections (6 mice). (For interpretation of the references to colour in this figure legend, the reader is referred to the web version of this article.)

0.0040; mean ± SEM: Vehicle = 9.922 ± 1.072; NRG-1 Treated = 17.28 ± 1.929), *s. radiatum* (t(df) = 3.460 (17), p = 0.0015; mean ± SEM: Vehicle = 9.209 ± 0.5827; NRG-1 Treated = 15.68 ± 1.525), *s. lacunosum moleculare* (t(df) = 2.913 (17), p = 0.0048; mean ± SEM: Vehicle = 8.334 ± 0.3993; NRG-1 Treated = 14.51 ± 1.772), the molecular layer (t(df) = 2.776 (17), p = 0.0065; mean ± SEM: Vehicle = 7.636 ± 0.2088; NRG-1 Treated = 14.69 ± 2.144), upper GCL (t(df) = 3.087 (17), p = 0.0033; mean ± SEM: Vehicle = 6.667 ± 0.3856; NRG-1 Treated = 12.08 ± 1.457), hilus (t(df) = 3.628 (17), p = 0.0010; mean ± SEM: Vehicle = 6.178 ± 0.2947; NRG-1 Treated = 14.15 ± 1.847), lower GCL (t(df) = 3.072 (17), p = 0.0035; mean ± SEM: Vehicle = 6.215 ± 0.4003; NRG-1 Treated = 11.84 ± 1.523), *s. pyramidale* of *CA3* (t(df) = 3.303 (17), p = 0.0021; mean ± SEM: Vehicle = 8.519 ± 0.3717; NRG-1 Treated = 16.76 ± 2.094), and *s. lucidum* (t(df) = 2.740 (17), p = 0.0070; mean ± SEM: Vehicle = 7.219 ± 0.2225; NRG-1 Treated = 12.83 ± 1.726) in NRG-1 treated mice in the contralateral hippocampus 7 days post-IHKA induced SE compared to vehicle (Fig. 9).

3.3. EAAC1 is downregulated post-IHKA induced SE

Hippocampal EAAC1 immunoreactivity was assessed at 7 days post-IHKA induced SE compared to saline-injected control animals. Quantification of individual hippocampal layers was performed for both hippocampi ipsilateral (Fig. 10) and contralateral (Fig. 11) to injection at 7 days post-IHKA induced SE. EAAC1 immunoreactivity was decreased in the ipsilateral hippocampus 7 days post-IHKA induced SE. Two-tailed *t*-tests on EAAC1 immunoreactivity of individual hippocampal layers in the ipsilateral hippocampus at 7 days post-IHKA revealed a main effect of treatment (Fig. 10). EAAC1 immunoreactivity was significantly decreased in *s. oriens* (t(df) = 4.295 (20), p = 0.0004; mean ± SEM: Saline = 37.72 ± 3.251; IHKA = 21.85 ± 2.018), *s. pyramidale* of *CA1* (t(df) = 2.792 (20), p = 0.0113; mean ± SEM: Saline = 35.59 ± 2.728; IHKA = 26.45 ± 1.943), *s. radiatum* (t(df) = 3.991 (20), p = 0.0007; mean ± SEM: Saline = 37.28 ± 3.207; IHKA = 22.86 ± 1.942) and *s. lacunosum moleculare* (t(df) = 3.871 (20), p = 0.0010; mean ± SEM: Saline = 41.09 ± 3.630; IHKA = 25.59 ± 2.067) in the ipsilateral hippocampus 7 days post-IHKA induced SE compared to saline injected control mice (Fig. 10). Two-tailed *t*-tests on EAAC1 immunoreactivity of individual hippocampal layers in the contralateral hippocampus at 7 days post-IHKA revealed no effect of treatment ($p > 0.05$) (Fig. 11).

3.4. EAAC1 is upregulated in mice treated with exogenous NRG-1 post-IHKA induced SE

EAAC1 immunoreactivity was increased in both hippocampi ipsilateral and contralateral to injection in NRG-1-treated mice *vs.* vehicle (Fig. 12, Fig. 13). One-tailed *t*-tests on EAAC1 immunoreactivity of individual hippocampal layers in the ipsilateral hippocampus at 7 days post-IHKA revealed a main effect of NRG-1 treatment (Fig. 12). EAAC1 immunoreactivity was significantly increased in *s. pyramidale* of *CA1* (t(df) = 1.849 (18), p = 0.0405; mean ± SEM: Vehicle = 21.86 ± 1.282; NRG-1 Treated = 26.08 ± 1.776) and the hilus (t(df) = 1.903 (18), p = 0.0366; mean ± SEM: Vehicle = 13.89 ± 0.6475; NRG-1 Treated = 20.87 ± 3.260) in NRG-1 treated mice in the ipsilateral hippocampus 7 days post-IHKA induced SE compared to vehicle.

One-tailed *t*-tests on EAAC1 immunoreactivity of individual hippocampal layers in the contralateral hippocampus at 7 days post-IHKA revealed a main effect of NRG-1 treatment (Fig. 13). EAAC1 immunoreactivity was significantly increased in *s. oriens* (t(df) = 1.941 (19), p = 0.0336; mean ± SEM: Vehicle = 29.31 ± 2.057; NRG-1 Treated = 39.96 ± 4.877), *s. pyramidale* of *CA1* (t(df) = 2.193 (19), p = 0.0205; mean ± SEM: Vehicle = 29.12 ± 0.9957; NRG-1 Treated = 38.52 ± 3.979), *s. radiatum* (t(df) = 2.528 (19), p = 0.0103; mean ± SEM: Vehicle = 28.68 ± 1.356; NRG-1 Treated = 40.65 ± 4.333), the molecular layer (t(df) = 1.790 (19), p = 0.0447; mean ± SEM: Vehicle = 30.39 ± 3.072; NRG-1 Treated = 39.73 ± 4.117), upper GCL (t(df) = 1.871 (19), p = 0.0384; mean ± SEM: Vehicle = 24.51 ± 2.660; NRG-1 Treated = 32.98 ± 3.570), hilus (t(df) = 1.903 (18), p = 0.0366; mean ± SEM: Vehicle = 13.89 ± 0.6475; NRG-1 Treated = 20.87 ± 3.260), lower GCL (t(df) = 2.524 (19), p = 0.0103; mean ± SEM: Vehicle = 21.43 ± 1.494; NRG-1 Treated = 32.50 ± 3.948), *s. pyramidale* of *CA3* (t(df) = 2.697 (19), p = 0.0071; mean ± SEM: Vehicle = 24.27 ± 1.760; NRG-1 Treated = 34.57 ± 3.264), and *s. lucidum* (t(df) = 2.267 (19), p = 0.0176; mean ± SEM: Vehicle = 16.10 ± 1.141; NRG-1 Treated = 22.89 ± 2.656) in NRG-1 treated mice in the contralateral hippocampus 7 days post-IHKA induced SE compared to vehicle (Fig. 13). NRG-1 treatment at 7 days post-IHKA induced SE selectively upregulated EAAC1 but not the glial glutamate transporters, EAAT1/GLAST and EAAT2/GLT-1 (Supplementary Fig. 1, Supplementary Fig. 2).

3.5. NeuN immunoreactivity in neurons is reduced post-IHKA induced SE

Hippocampal NeuN immunoreactivity was assessed at 7 post-IHKA-induced SE compared to saline-injected control animals (Fig. 14, Fig. 15). Quantification of NeuN immunoreactivity was examined in *s. pyramidale* of *CA1*, dentate gyrus, and *s. pyramidale* of *CA3* for hippocampi both ipsilateral (Fig. 14) and contralateral (Fig. 15) to injection. NeuN immunoreactivity was decreased in both hippocampi ipsilateral and contralateral to injection compared to saline-injected control animals. Two-tailed *t*-tests on NeuN immunoreactivity in the ipsilateral hippocampus revealed a main effect of treatment in *s. pyramidale* of *CA1* (t(df) = 5.919 (22), p < 0.0001; mean ± SEM: Saline = 2163 ± 220.6; IHKA = 832.9 ± 42.87), the dentate gyrus (t(df) = 3.232 (21), p = 0.0040; mean ± SEM: Saline = 3939 ± 388.9; IHKA = 2451 ± 224.9), and *s. pyramidale* of *CA3* (t(df) = 5.872 (22), p < 0.0001; mean ± SEM: Saline = 3990 ± 348.2; IHKA = 1670 ± 186.7). Two-tailed *t*-tests on NeuN immunoreactivity in the contralateral hippocampus revealed a main effect of treatment in *s. pyramidale* of *CA1* (t(df) = 3.934 (21), p = 0.0008; mean ± SEM: Saline = 2211 ± 179.7; IHKA = 1357 ± 113.5), the dentate gyrus (t(df) = 2.223 (20), p = 0.0379; mean ± SEM: Saline = 4005 ± 374.9; IHKA = 2901 ± 304.9), and *s. pyramidale* of *CA3* (t(df) = 3.647 (21), p = 0.0015; mean ± SEM: Saline = 4259 ± 418.5; IHKA = 2429 ± 256.3).

3.6. Exogenous NRG-1 treatment is neuroprotective at early time points during the development of epilepsy

Hippocampal NeuN immunoreactivity was assessed at 7 post-IHKA-induced SE in NRG-1 treated mice *vs.* vehicle (Fig. 16, Fig. 17). Quantification of NeuN immunoreactivity was examined in *s. pyramidale* of *CA1*, dentate gyrus, and *s. pyramidale* of *CA3* for hippocampi both ipsilateral (Fig. 16) and contralateral (Fig. 17) to injection. NeuN immunoreactivity was increased in NRG-1 treated mice in both hippocampi ipsilateral and contralateral to injection compared to vehicle. Two-tailed t-tests on NeuN immunoreactivity in the ipsilateral hippocampus revealed a main effect of NRG-1 treatment in the dentate gyrus (t(df) = 2.489 (16), p = 0.0242; mean ± SEM: Vehicle = 2455 ± 228.4;

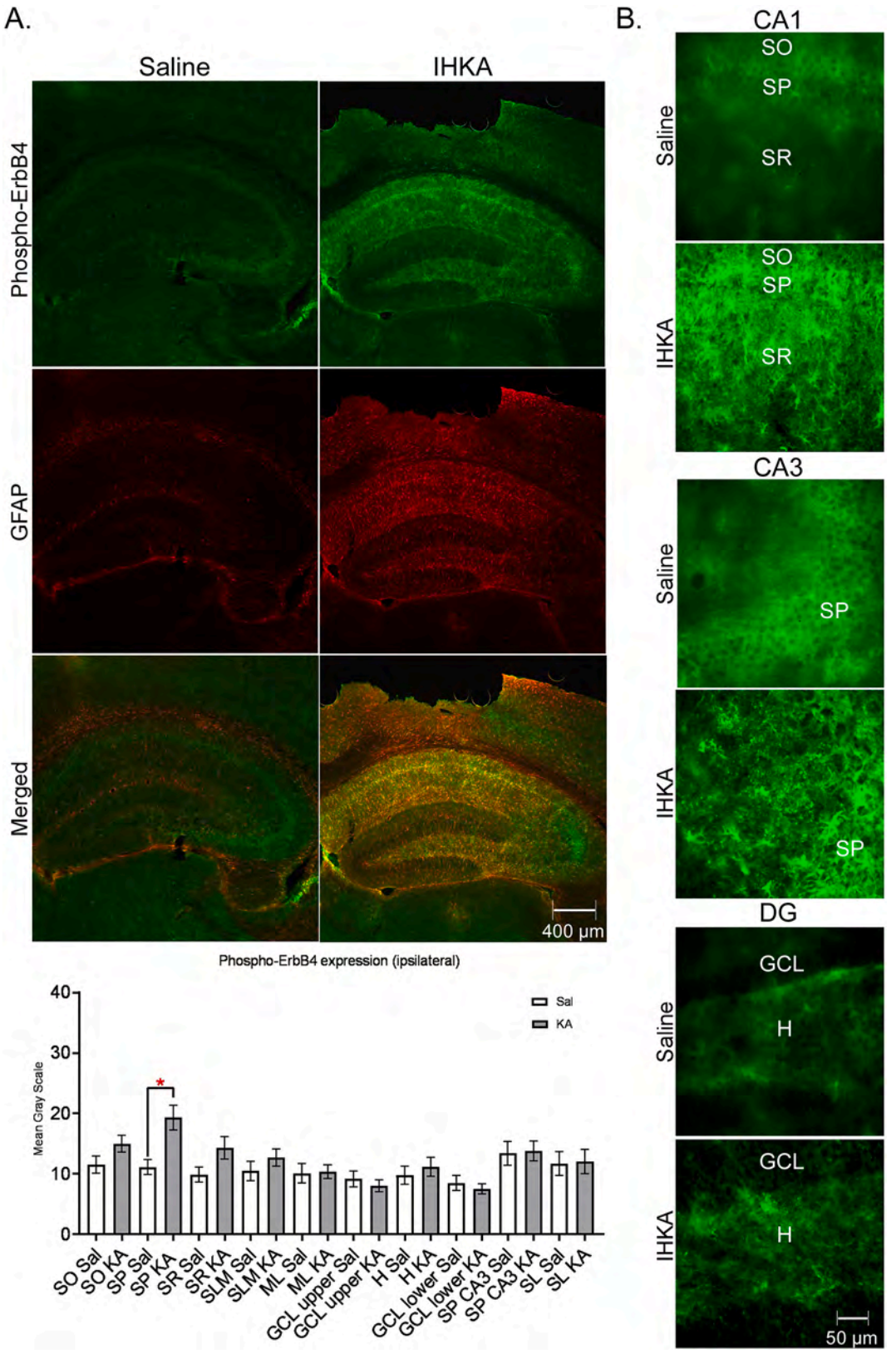

Fig. 4. Phospho-ErbB4 expression is increased in the ipsilateral hippocampus 7 days post-IHKA induced SE. A. Phospho-ErbB4 (green) and GFAP (red) expression in the ipsilateral hippocampus 7 days post-IHKA induced SE *vs.* saline-injected control mice (5×). Phospho-ErbB4 mean gray scale quantitation of individual cell layers. B. Phospho-ErbB4 expression in CA1, CA3 and DG at 7 days post-IHKA induced SE (40×). SO = *Stratum Oriens*; SP = *Stratum Pyramidale*; SR = *Stratum Radiatum*; SLM = *Stratum Lacunosum Moleculare*; GCL = Granule Cell Layer; H = Hilus SL = *Stratum Lucidum*. Saline group; N = 8 sections (4 mice). IHKA group; N = 10 sections (5 mice). (For interpretation of the references to colour in this figure legend, the reader is referred to the web version of this article.)

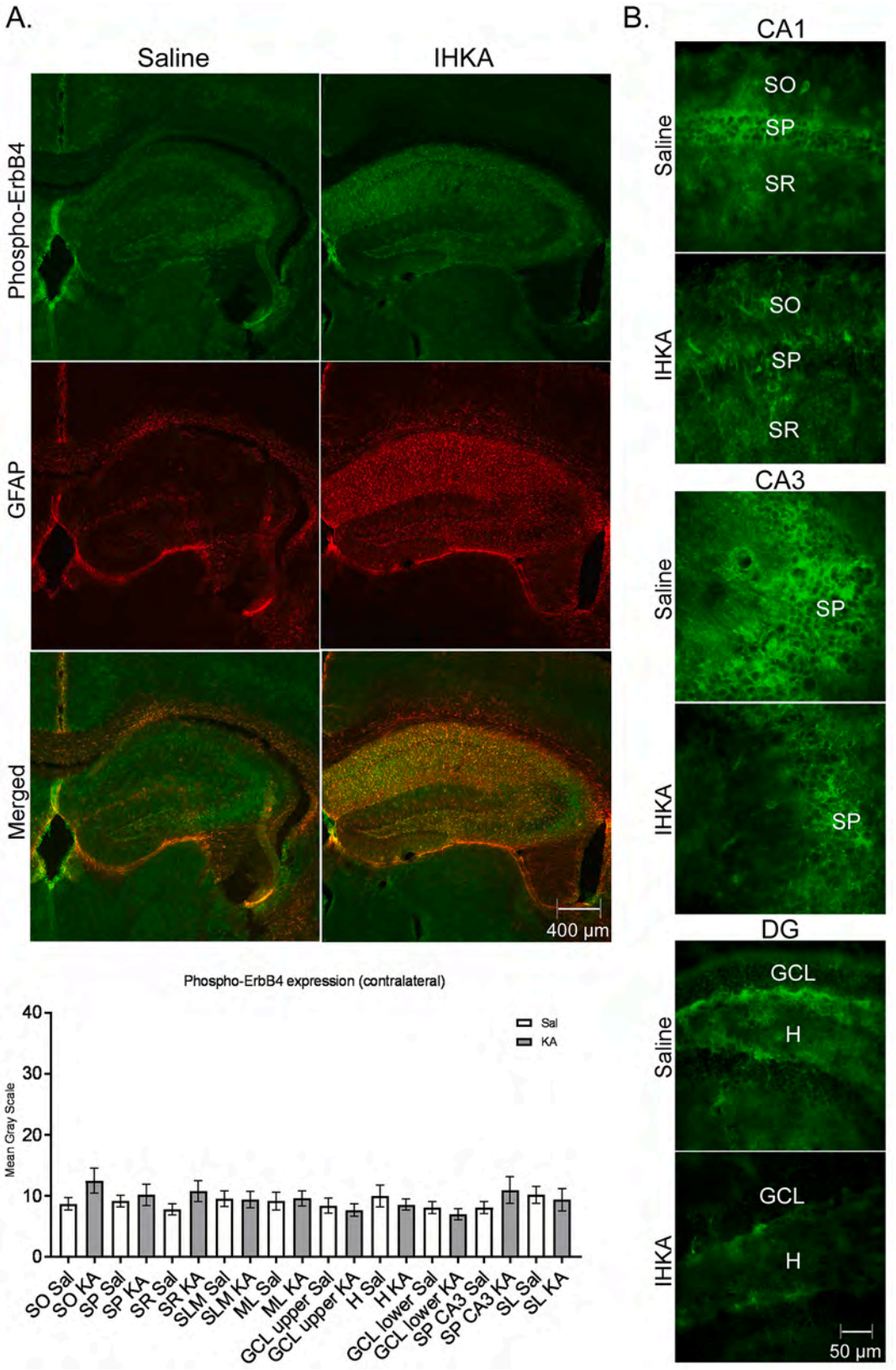

Fig. 5. Phospho-ErbB4 expression in the contralateral hippocampus 7 days post-IHKA induced SE. A. Phospho-ErbB4 (green) and GFAP (red) expression in the contralateral hippocampus 7 days post-IHKA induced SE *vs.* saline injected control mice (5×). Phospho-ErbB4 mean gray scale quantitation of individual cell layers. B. Phospho-ErbB4 expression in CA1, CA3 and DG at 7 days post-IHKA induced SE (40×). SO = *Stratum Oriens*; SP = *Stratum Pyramidale*; SR = *Stratum Radiatum*; SLM = *Stratum Lacunosum Moleculare*; GCL = Granule Cell Layer; H = Hilus SL = *Stratum Lucidum*. Saline group; N = 6 sections (4 mice). IHKA group; N = 9 sections (5 mice). (For interpretation of the references to colour in this figure legend, the reader is referred to the web version of this article.)

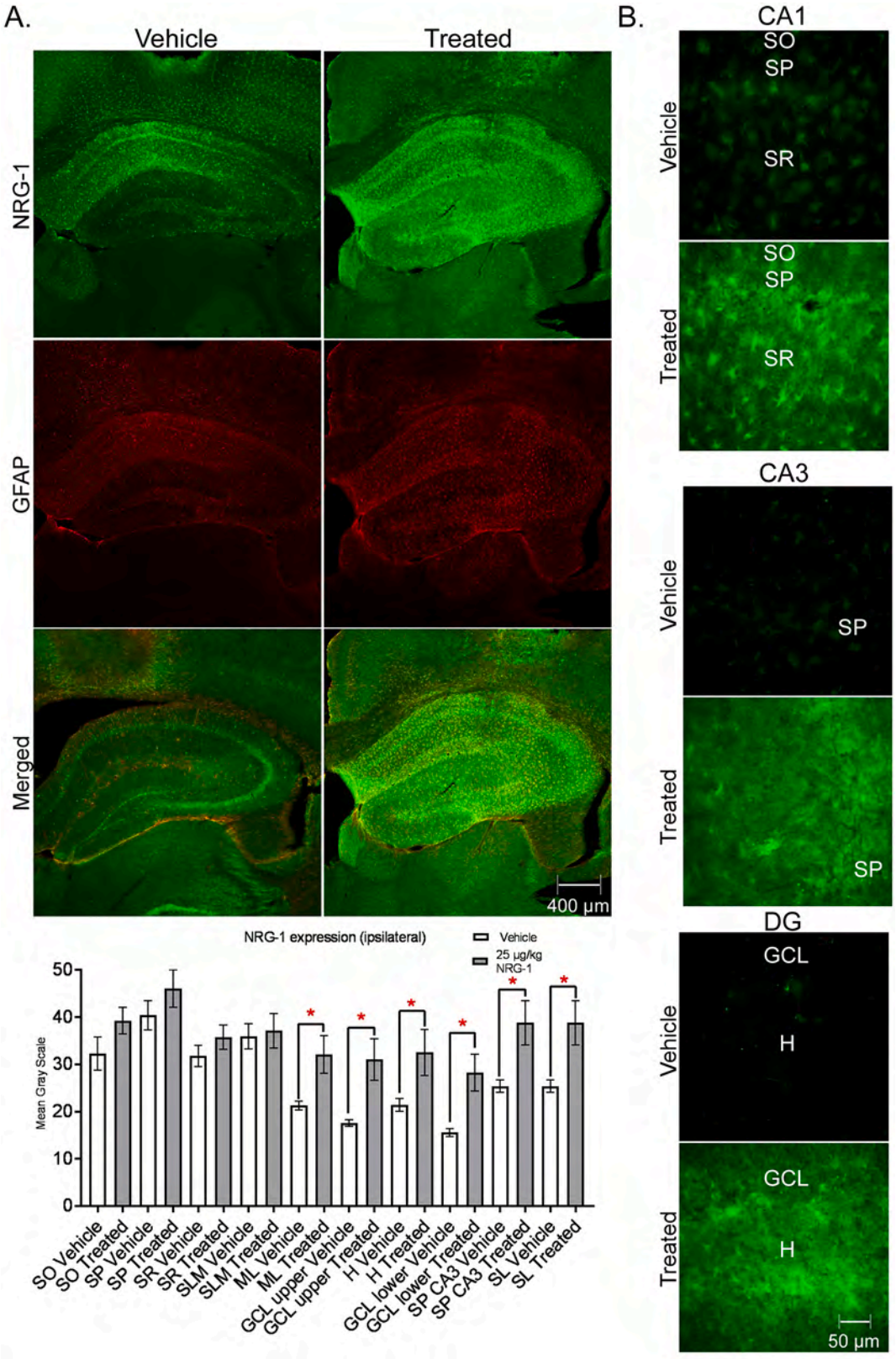

Fig. 6. Neuregulin-1 (NRG-1) expression is increased in the ipsilateral hippocampus of mice treated with 25 μg/kg NRG-1 at 7 days post-IHKA induced SE. A. NRG-1 (green) and GFAP (red) expression in the ipsilateral hippocampus of NRG-1 treated *vs.* vehicle-treated mice at 7 days post-IHKA induced SE (5×). NRG-1 mean gray scale quantitation of individual cell layers. B. NRG-1 expression in CA1, CA3 and DG at 7 days post-IHKA induced SE (40×). SO = Stratum Oriens; SP = *Stratum Pyramidale*; SR = *Stratum Radiatum*; SLM = *Stratum Lacunosum Moleculare*; GCL = Granule Cell Layer; H = Hilus; SL = *Stratum Lucidum*. Vehicle group; N = 9 sections (5 mice). NRG-1 Treatment group; N = 11 sections (6 mice). (For interpretation of the references to colour in this figure legend, the reader is referred to the web version of this article.)

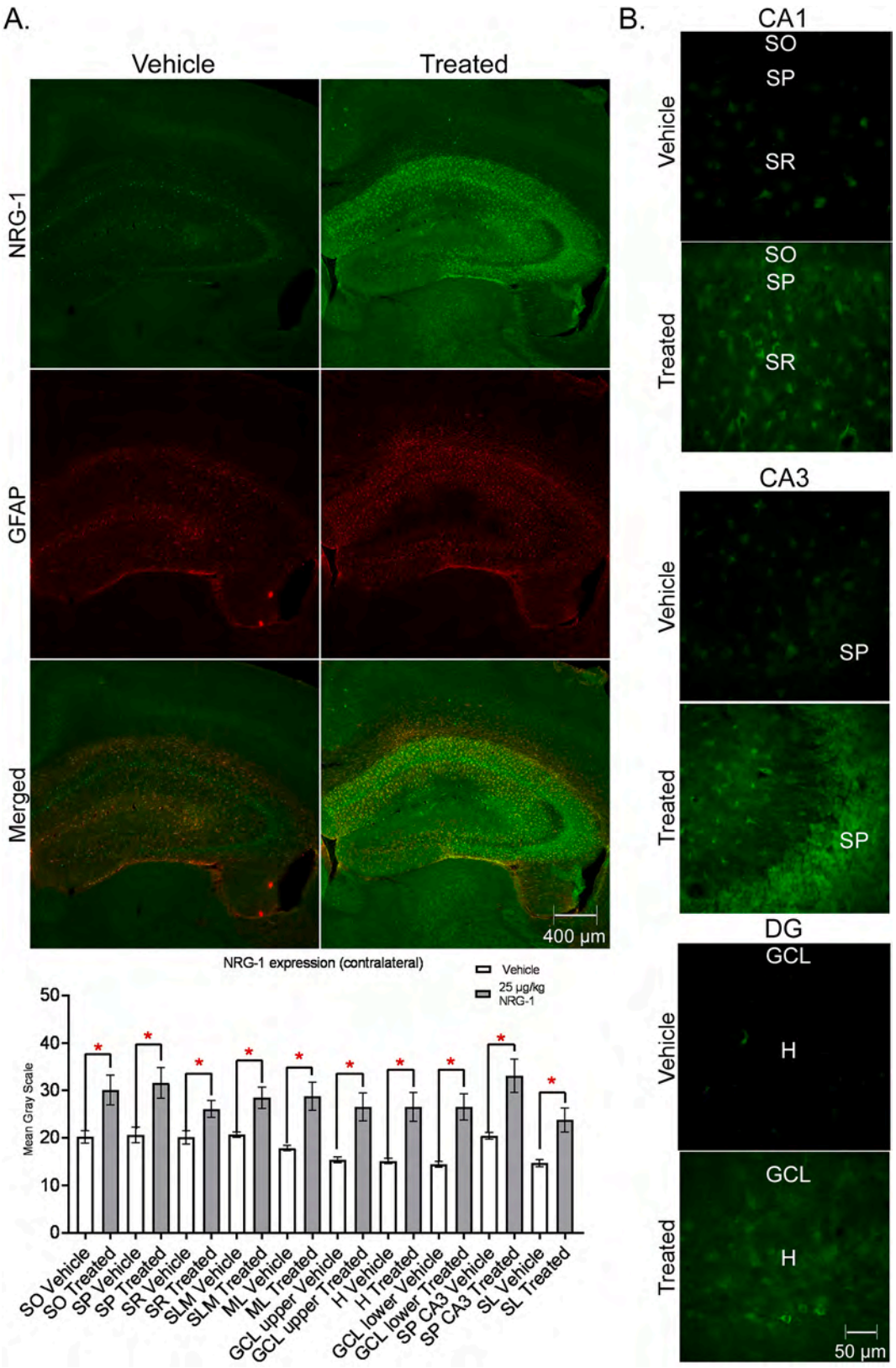

Fig. 7. Neuregulin-1 (NRG-1) expression is increased in the contralateral hippocampus of mice treated with 25 μg/kg NRG-1 at 7 days post-IHKA induced SE. A. NRG-1 (green) and GFAP (red) expression in the contralateral hippocampus of NRG-1-treated *vs.* vehicle-treated mice at 7 days post-IHKA induced SE (5×). NRG-1 mean gray scale quantitation of individual cell layers. B. NRG-1 expression in CA1, CA3 and DG at 7 days post-IHKA induced SE (40×). SO = *Stratum Oriens*; SP = *Stratum Pyramidale*; SR = *Stratum Radiatum*; SLM = *Stratum Lacunosum Moleculare*; GCL = Granule Cell Layer; H = Hilus; SL = *Stratum Lucidum*. Vehicle group; N = 10 sections (5 mice). NRG-1 Treatment group; N = 11 sections (6 mice). (For interpretation of the references to colour in this figure legend, the reader is referred to the web version of this article.)

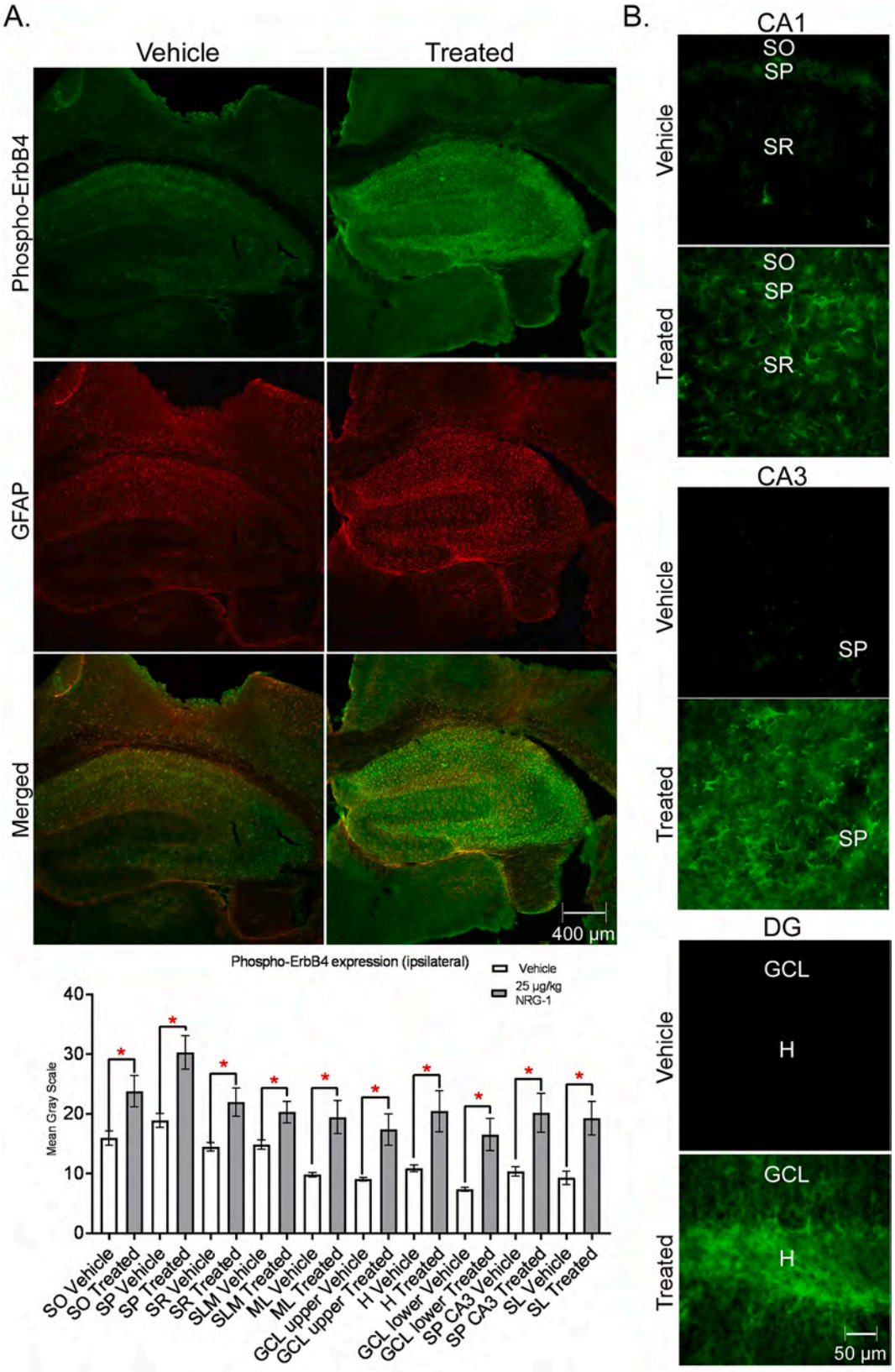

Fig. 8. Phospho-ErbB4 expression is increased in the ipsilateral hippocampus of mice treated with 25 μg/kg NRG-1 7 days post-IHKA induced SE. A. Phospho-ErbB4 (green) and GFAP (red) expression in the ipsilateral hippocampus of NRG-1-treated *vs.* vehicle-treated mice at 7 days post-IHKA induced SE (5×). Phospho-ErbB4 mean gray scale quantitation of individual cell layers. B. Phospho-ErbB4 expression in CA1, CA3 and DG at 7 days post-IHKA induced SE (40×). SO = *Stratum Oriens*; SP = *Stratum Pyramidale*; SR = *Stratum Radiatum*; SLM = *Stratum Lacunosum Moleculare*; GCL = Granule Cell Layer; H = Hilus; SL = *Stratum Lucidum*. Vehicle group; N = 8 sections (4 mice). NRG-1 Treatment group; N = 9 sections (5 mice). (For interpretation of the references to colour in this figure legend, the reader is referred to the web version of this article.)

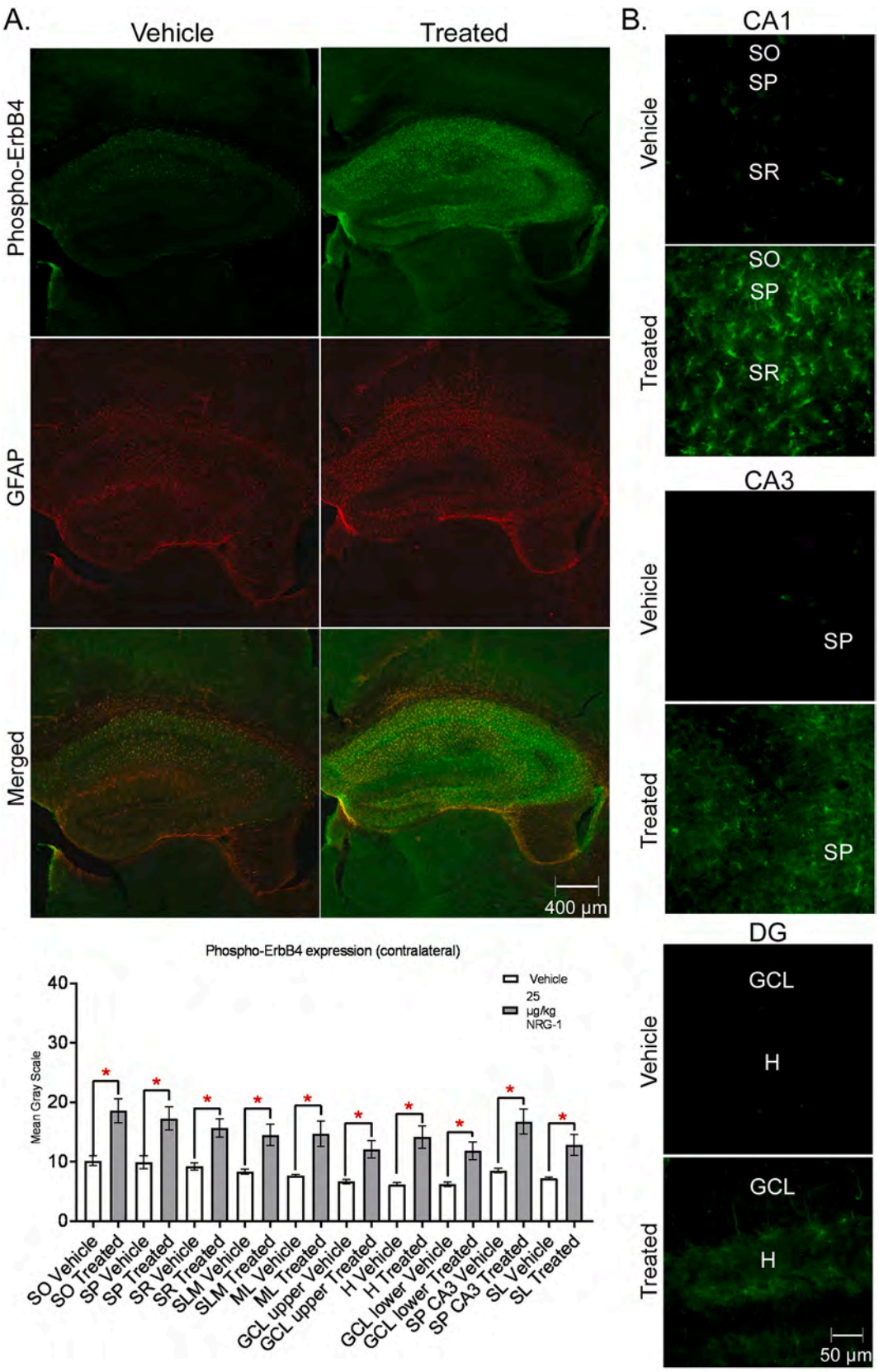

Fig. 9. Phospho-ErbB4 expression is increased in the contralateral hippocampus of mice treated with 25 μg/kg NRG-1 7 days post-IHKA induced SE. A. Phospho-ErbB4 (green) and GFAP (red) expression in the contralateral hippocampus of NRG-1-treated *vs.* vehicle-treated mice at 7 days post-IHKA induced SE (5×). Phospho-ErbB4 mean gray scale quantitation of individual cell layers. B. Phospho-ErbB4 expression in CA1, CA3 and DG at 7 days post-IHKA (40×). SO = Stratum Oriens; SP = Stratum Pyramidale; SR = *Stratum Radiatum*; SLM = *Stratum Lacunosum Moleculare*; GCL = Granule Cell Layer; H = Hilus; SL = *Stratum Lucidum*. Vehicle group; N = 8 sections (4 mice). NRG-1 Treatment group; N = 11 sections (6 mice). (For interpretation of the references to colour in this figure legend, the reader is referred to the web version of this article.)

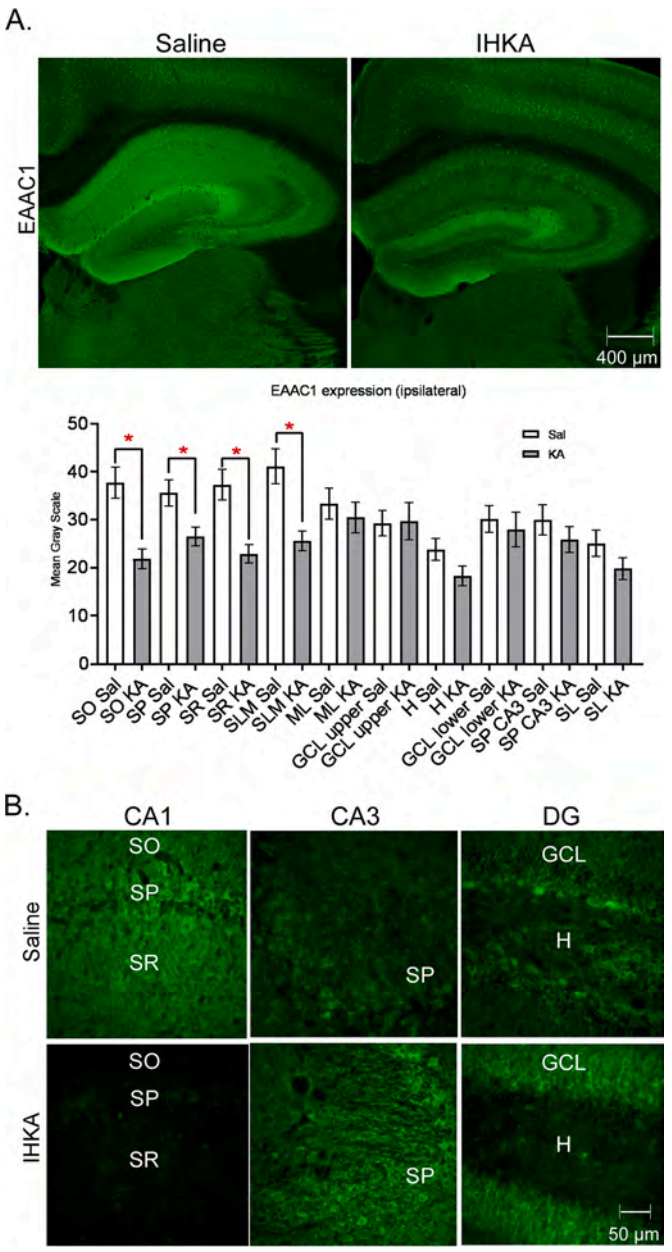

Fig. 10. EAAC1 expression is decreased in the ipsilateral hippocampus 7 days post-IHKA induced SE. A. EAAC1 (green) expression in the ipsilateral hippocampus 7 days post-IHKA induced SE *vs.* saline-injected control mice (5×). EAAC1 mean gray scale quantitation of individual cell layers. B. EAAC1 expression in CA1, CA3 and DG at 7 days post-IHKA induced SE (40×). SO = *Stratum Oriens*; SP = *Stratum Pyramidale*; SR = *Stratum Radiatum*; SO = *Stratum Oriens*; SP = *Stratum Pyramidale*; SR = *Stratum Radiatum*; SLM = *Stratum Lacunosum Moleculare*; GCL = Granule Cell Layer; H = Hilus; SL = *Stratum Lucidum*. Saline group; N = 10 sections (6 mice). IHKA group; N = 12 sections (6 mice). (For interpretation of the references to colour in this figure legend, the reader is referred to the web version of this article.)

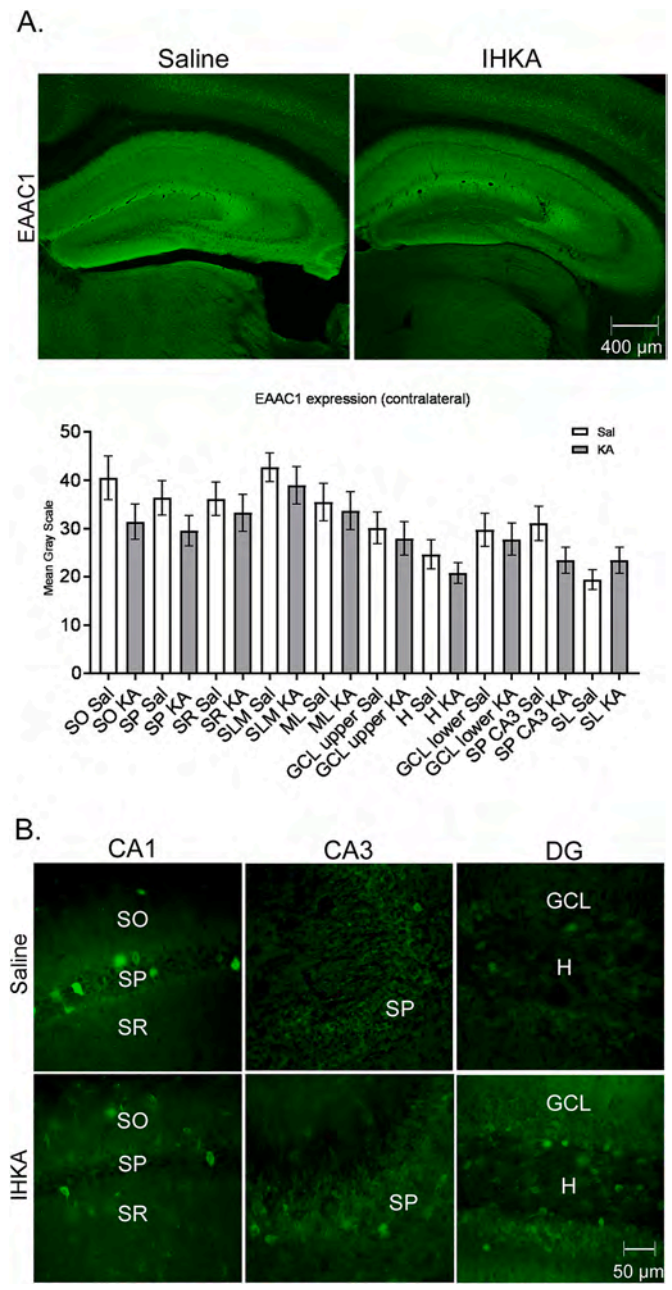

Fig. 11. EAAC1 expression in the contralateral hippocampus 7 days post-IHKA induced SE. A. EAAC1 (green) expression in the contralateral hippocampus 7 days post-IHKA induced SE *vs.* saline-injected control mice (5×). EAAC1 mean gray scale quantitation of individual cell layers. B. EAAC1 expression in CA1, CA3 and DG at 7 days post-IHKA induced SE (40×). SO = *Stratum Oriens*; SP = *Stratum Pyramidale*; SR = *Stratum Radiatum*; SLM = *Stratum Lacunosum Moleculare*; GCL = Granule Cell Layer; H = Hilus; SL = *Sratum Lucidum*. Saline group; N = 10 sections (6 mice). IHKA group; N = 12 sections (6 mice). (For interpretation of the references to colour in this figure legend, the reader is referred to the web version of this article.)

NRG-1 Treated = 3662 ± 428.0). Two-tailed t-tests on NeuN immunoreactivity in the contralateral hippocampus revealed a main effect of NRG-1 treatment in the dentate gyrus (t(df) = 3.870 (18), p = 0.0011; mean ± SEM: Vehicle = 2751 ± 164.2; NRG-1 Treated = 4871 ± 522.6) and *s. pyramidale* of *CA3* (t(df) = 3.001 (19), p = 0.0074; mean ± SEM: Vehicle = 2502 ± 124.6; NRG-1 Treated = 3882 ± 422.8). NRG-1/ErbB4 activity has been shown to modulate EAAC1 (Yu et al., 2015). Hippocampal parvalbumin immunoreactivity was also assessed at 7 post-IHKA-induced SE in NRG-1 treated mice *vs.* vehicle (Fig. 18). Two-tailed *t*-tests on parvalbumin immunoreactivity in the hippocampi ipsilateral and contralateral to injection revealed no effect of NRG-1 treatment at 7 days post-IHKA induced SE ($p > 0.05$).

GFAP is upregulated in mice treated with exogenous NRG-1 post-IHKA induced SE.

NRG-1, phospho-ErbB4 and EAAC1 immunoreactivity was assessed with either glial fibrillary acidic protein (GFAP) or NeuN immunoreactivity to determine which cell types were expressing these three proteins (Fig. 19). We observed co-localization of NRG-1/ErbB4 activity in

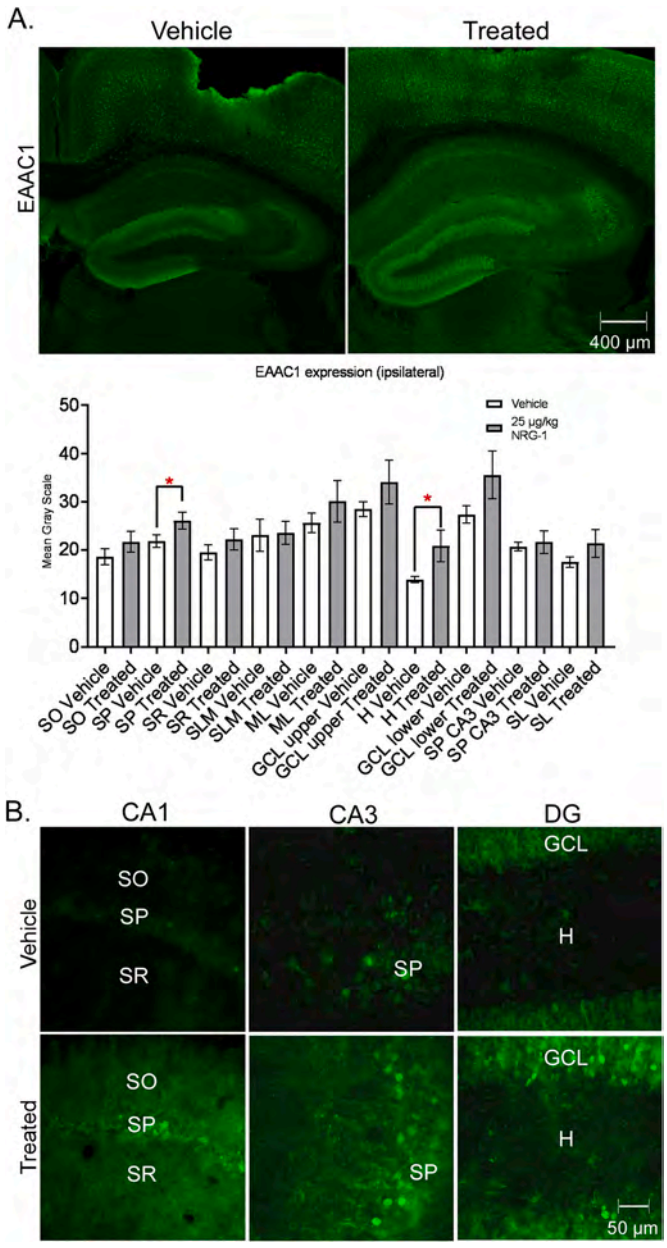

Fig. 12. EAAC1 expression is increased in the ipsilateral hippocampus of mice treated with 25 μg/kg NRG-1 7 days post-IHKA induced SE. A. EAAC1 (green) in the ipsilateral hippocampus of NRG-1-treated *vs.* vehicle-treated mice at 7 days post-IHKA induced SE (5×). EAAC1 mean gray scale quantitation of individual cell layers. B. EAAC1 expression in CA1, CA3 and DG at 7 days post-IHKA induced SE (40×). SO = *Stratum Oriens*; SP = *Stratum Pyramidale*; SR = *Stratum Radiatum*; SLM = *Stratum Lacunosum Moleculare*; GCL = Granule Cell Layer; H = Hilus; SL = *Stratum Lucidum*. Vehicle group; N = 9 sections (5 mice). NRG-1 Treatment group; N = 11 sections (6 mice). (For interpretation of the references to colour in this figure legend, the reader is referred to the web version of this article.)

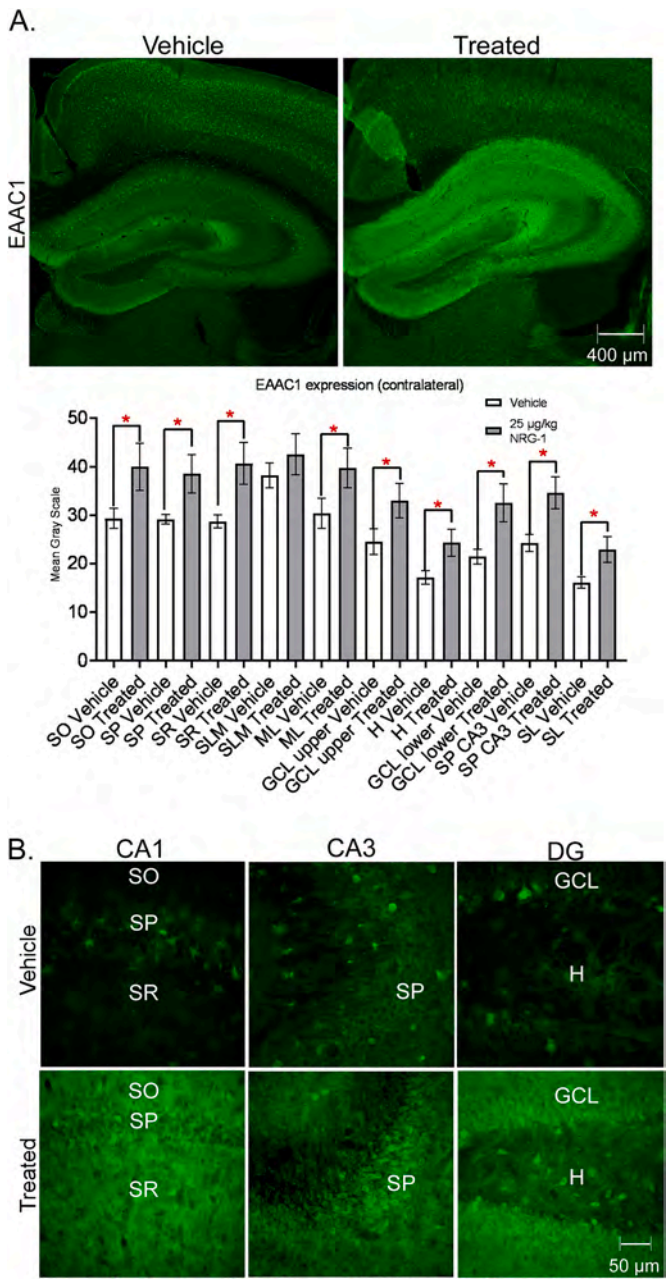

Fig. 13. EAAC1 expression is increased in the contralateral hippocampus of mice treated with 25 μg/kg NRG-1 7 days post-IHKA induced SE. A. EAAC1 (green) expression in the contralateral hippocampus of NRG-1-treated *vs.* vehicle-treated mice at 7 days post-IHKA induced SE (5×). EAAC1 mean gray scale quantitation of individual cell layers. B. EAAC1 expression in CA1, CA3 and DG at 7 days post-IHKA (40×). SO = *Stratum Oriens*; SP = *Stratum Pyramidale*; SR = *Stratum Radiatum*; SLM = *Stratum Lacunosum Moleculare*; GCL = Granule Cell Layer; H = Hilus SL = *Stratum Lucidum*. Vehicle group; N = 10 sections (5 mice). NRG-1 Treatment group; N = 11 sections (6 mice). (For interpretation of the references to colour in this figure legend, the reader is referred to the web version of this article.)

GFAP+ cells and co-localization with EAAC1 and NeuN immunohistochemistry. GFAP immunoreactivity was increased in both hippocampi ipsilateral and contralateral to injection in NRG-1 treated mice *vs.* vehicle (Fig. 20). Two-tailed *t*-tests on GFAP immunoreactivity of individual hippocampal layers in the ipsilateral hippocampus at 7 days post-IHKA revealed a main effect of NRG-1 treatment. GFAP immunoreactivity was significantly increased in the molecular layer (t(df) = 3.676 (18), p = 0.0017; mean ± SEM: Vehicle = 15.05 ± 0.5260; NRG-1 Treated = 18.06 ± 0.6019), upper GCL (t(df) = 2.467 (18), p = 0.0239; mean ± SEM: Vehicle = 11.30 ± 1.101; NRG-1 Treated = 14.27 ± 0.6142), lower GCL (t(df) = 4.505 (18), p = 0.0003; mean ± SEM: Vehicle = 9.582 ± 0.7570; NRG-1 Treated = 14.76 ± 0.8346), *s. pyramidale* of *CA3* (t(df) = 3.252 (18), p = 0.0044; mean ± SEM: Vehicle = 9.035 ± 0.7866; NRG-1 Treated = 14.13 ± 1.257), and *s. lucidum* (t(df) = 2.754 (18), p = 0.0131; mean ± SEM: Vehicle = 9.971 ± 0.7079; NRG-1 Treated = 13.31 ± 0.9289) in NRG-1 treated mice in the ipsilateral hippocampus 7 days post-IHKA induced SE compared to vehicle.

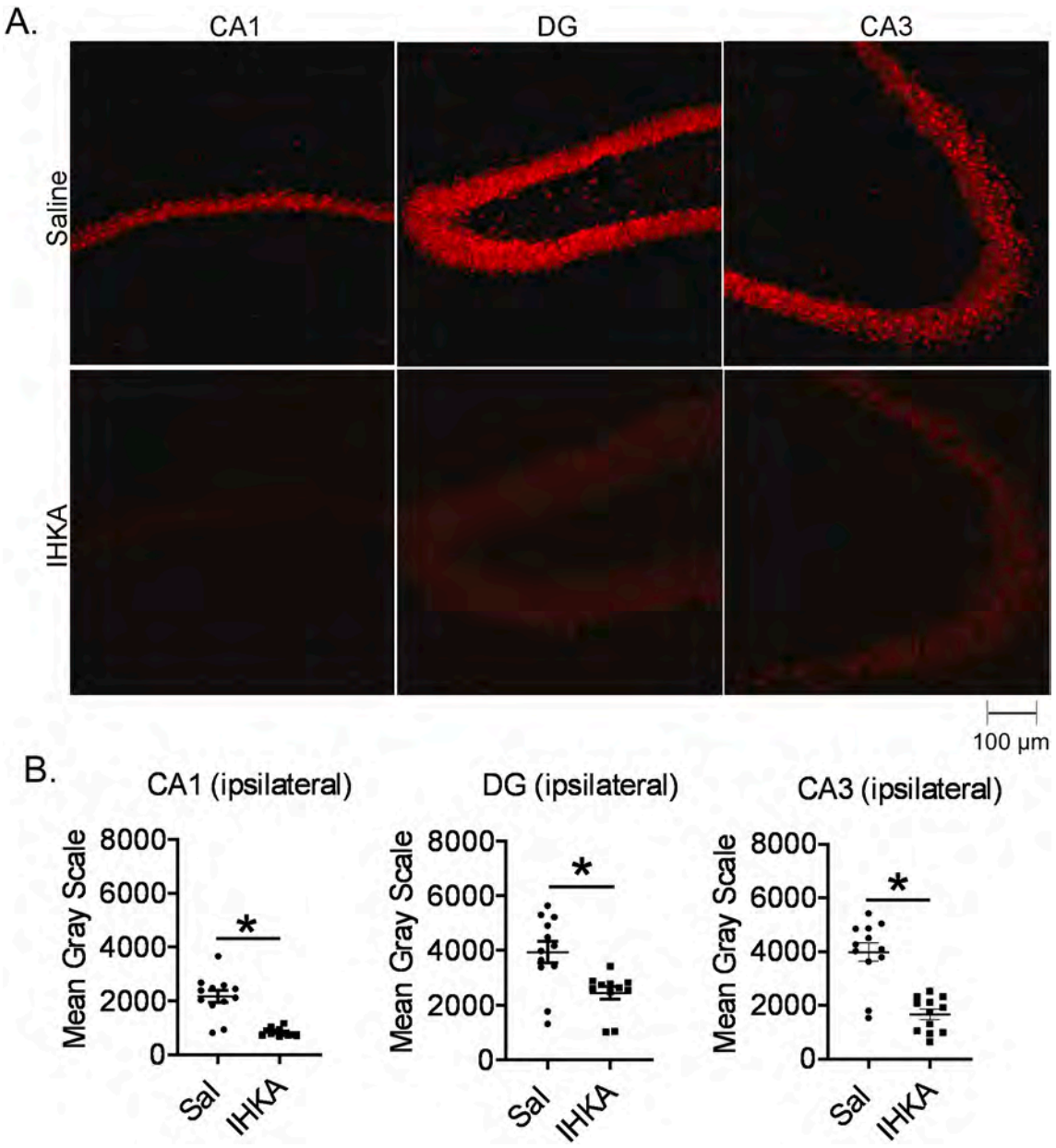

Fig. 14. NeuN immunoreactivity is decreased 7 days post-IHKA induced SE in the ipsilateral hippocampus. Coronal section of the ipsilateral hippocampus 7 days post-IHKA induced SE showing expression and quantitation of NeuN immunoreactivity in hippocampal CA1, DG, and CA3 compared to saline-injected control mice. Saline group; N = 12 sections (6 mice). IHKA group; N = 11 sections (6 mice) (20×).

GFAP immunoreactivity was significantly increased in the lower GCL (t (df) = 2.214 (18), p = 0.0380; mean ± SEM: Vehicle = 8.886 ± 0.4332; NRG-1 Treated = 14.61 ± 2.665) in NRG-1 treated mice in the contralateral hippocampus 7 days post-IHKA induced SE compared to vehicle (Fig. 20).

3.7. Glutamine synthetase (GS) is upregulated in mice treated with exogenous NRG-1 post-IHKA induced SE

Glutamine synthetase (GS) immunoreactivity was increased in both hippocampi ipsilateral and contralateral to injection in NRG-1 treated mice *vs.* vehicle (Fig. 21, Fig. 22). Two-tailed *t*-tests on GS immunoreactivity of individual hippocampal layers in the ipsilateral hippocampus at 7 days post-IHKA revealed a main effect of NRG-1 treatment in all layers (Fig. 21). GS immunoreactivity was significantly increased in *s. oriens* (t(df) = 5.528 (20), p < 0.0001; mean ± SEM: Vehicle = 18.05 ± 0.8676; NRG-1 Treated = 24.86 ± 0.8589), *s. radiatum* (t(df) = 6.225 (20), p < 0.0001; mean ± SEM: Vehicle = 19.72 ± 0.6287; NRG-1 Treated = 25.99 ± 0.7541), *s. lacunosum moleculare* (t(df) = 4.255 (20), p = 0.0004; mean ± SEM: Vehicle = 20.51 ± 1.119; NRG-1 Treated = 27.72 ± 1.234), the molecular layer (t(df) = 6.576 (20), p < 0.0001; mean ± SEM: Vehicle = 17.34 ± 0.7620; NRG-1 Treated = 24.66 ± 0.7929), lower GCL (t(df) = 2.582 (20), p = 0.0178; mean ± SEM: Vehicle = 7.280 ± 0.5675; NRG-1 Treated = 11.02 ± 1.232), *s. pyramidale* of *CA3* (t(df) = 4.714 (20), p = 0.0001; mean ± SEM: Vehicle = 12.26 ± 0.7823; NRG-1 Treated = 20.74 ± 1.502), and *s. lucidum* (t (df) = 3.892 (20), p = 0.0009; mean ± SEM: Vehicle = 10.72 ± 0.4736; NRG-1 Treated = 17.06 ± 1.429) in NRG-1 treated mice in the ipsilateral hippocampus 7 days post-IHKA induced SE compared to vehicle (Fig. 21).

Two-tailed t-tests on GS immunoreactivity of individual hippocampal layers in the contralateral hippocampus at 7 days post-IHKA

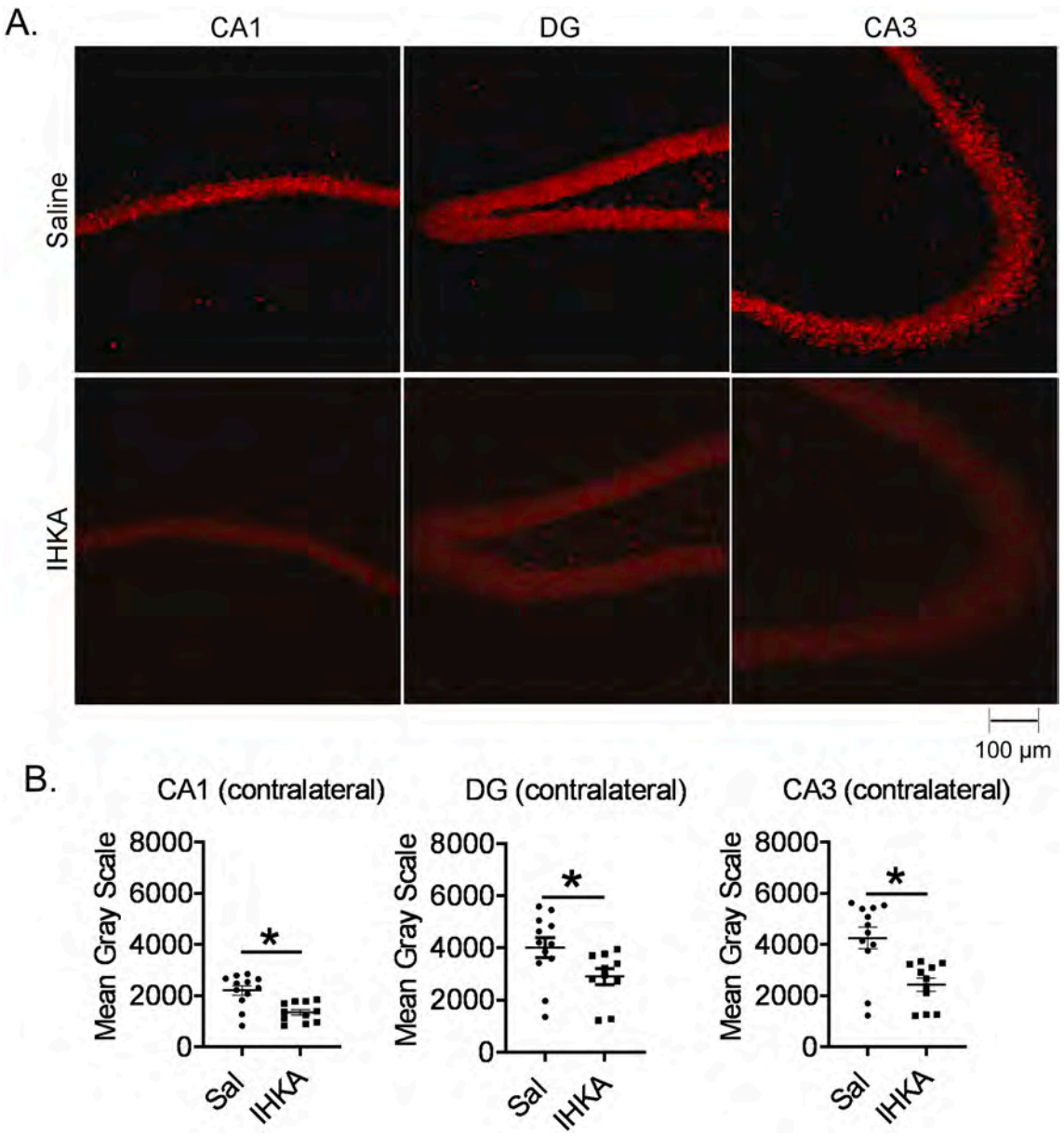

Fig. 15. NeuN immunoreactivity is decreased 7 days post-IHKA induced SE in the contralateral hippocampus. Coronal section of the contralateral hippocampus 7 days post-IHKA induced SE showing expression and quantitation of NeuN immunoreactivity in CA1, DG, and CA3 compared to saline-injected control mice. Saline group; N = 12 sections (6 mice). IHKA group; N = 10 sections (6 mice) (20×).

revealed a main effect of NRG-1 treatment (Fig. 21). GS immunoreactivity was significantly increased in *s. oriens* (t(df) = 3.658 (20), p = 0.0016; mean ± SEM: Vehicle = 19.95 ± 0.7489; NRG-1 Treated = 24.83 ± 1.044), *s. radiatum* (t(df) = 3.120 (20), p = 0.0054; mean ± SEM: Vehicle = 19.01 ± 1.019; NRG-1 Treated = 23.41 ± 0.9657), *s. lacunosum moleculare* (t(df) = 3.169 (20), p = 0.0048; mean ± SEM: Vehicle = 12.25 ± 0.8908; NRG-1 Treated = 18.60 ± 1.669), the molecular layer (t(df) = 2.356 (20), p = 0.0288; mean ± SEM: Vehicle = 11.75 ± 1.776; NRG-1 Treated = 18.23 ± 2.029), upper GCL (t(df) = 2.939 (20), p = 0.0081; mean ± SEM: Vehicle = 7.336 ± 0.6185; NRG-1 Treated = 13.27 ± 1.763), hilus (t(df) = 4.793 (20), p = 0.0001; mean ± SEM: Vehicle = 9.519 ± 0.9616; NRG-1 Treated = 17.47 ± 1.282), lower GCL (t(df) = 4.467 (20), p = 0.0002; mean ± SEM: Vehicle = 6.978 ± 0.3290; NRG-1 Treated = 11.18 ± 0.8109), *s. pyramidale* of *CA3* (t(df) = 4.203 (20), p = 0.0004; mean ± SEM: Vehicle = 14.05 ± 0.8694; NRG-1 Treated = 19.32 ± 0.8843), and *s. lucidum* (t(df) = 2.630 (20), p = 0.0161; mean ± SEM: Vehicle = 15.29 ± 0.7896; NRG-1 Treated = 18.13 ± 0.7343) in NRG-1 treated mice in the contralateral hippocampus 7 days post-IHKA induced SE compared to vehicle (Fig. 21).

4. Discussion

In this study, we used immunohistochemistry to demonstrate that NRG/ErbB4 signaling is increased, EAAC1 protein levels are downregulated, and NeuN immunoreactivity is decreased in epileptogenesis while exogenous NRG-1 (25 µg/kg/day) treatment increases NRG/ErbB4 activity, is neuroprotective, upregulates glutamate transporter EAAC1, and induces upregulation of GFAP in the IHKA model of epilepsy. This is the first paper to demonstrate that neuronal glutamate transporter EAAC1 is dysregulated in epileptogenesis and daily treatment with high dose NRG-1 (25 µg/kg) rescues EAAC1 and is neuroprotective during the development of epilepsy. To our knowledge, we are also the first to demonstrate that NRG-1/ErbB4 signaling in astrocytes increases levels of glutamine synthetase, an essential enzyme in

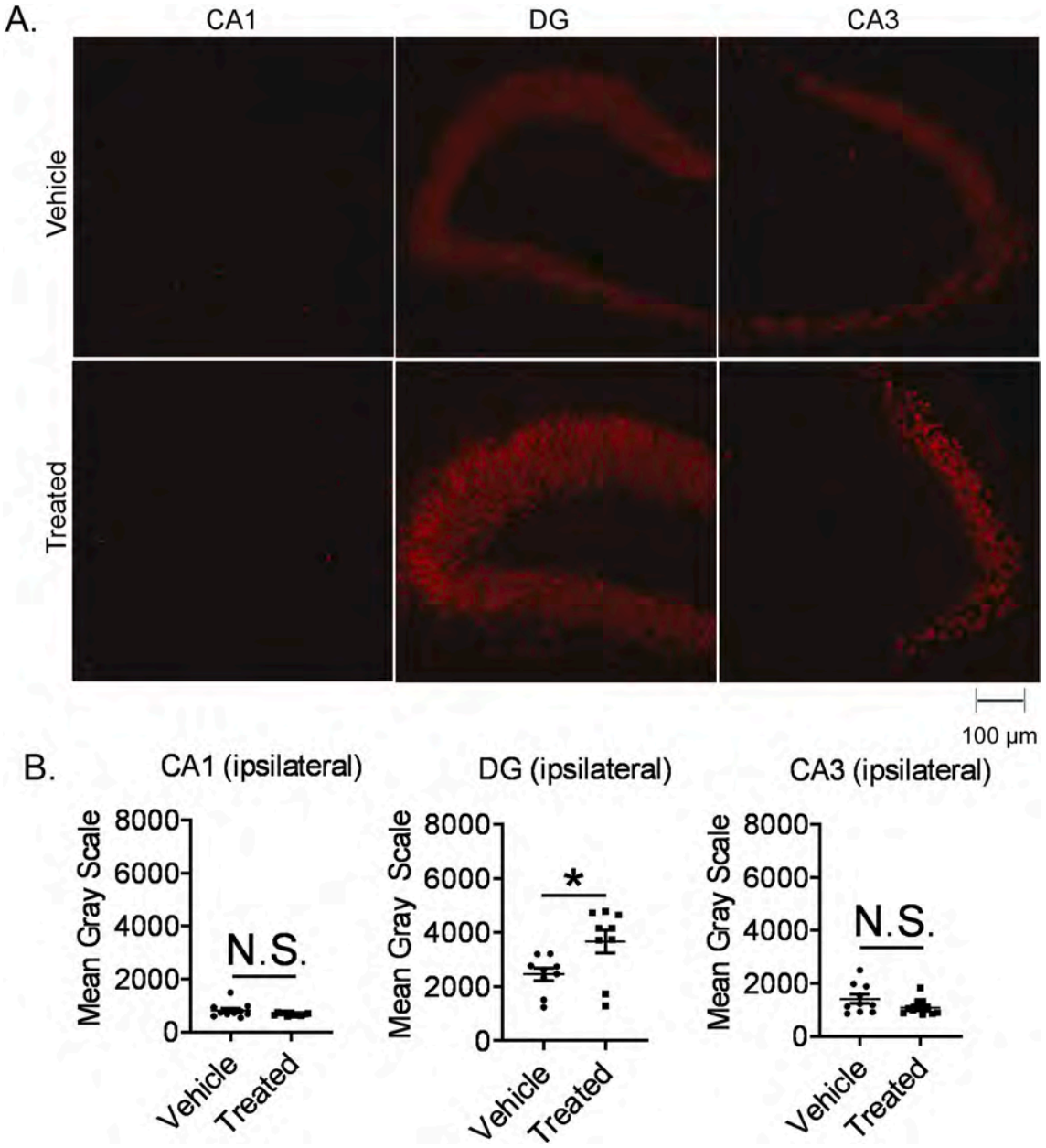

Fig. 16. NeuN immunoreactivity is increased 7 days post-IHKA induced SE in the ipsilateral hippocampus of NRG-1 treated mice. Coronal section of the ipsilateral hippocampus 7 days post-IHKA induced SE showing expression and quantitation of NeuN immunoreactivity in CA1, DG, and CA3 of NRG-1 treated mice *vs.* vehicle. Vehicle group; N = 9 sections (5 mice). NRG-1 Treatment group; N = 9 sections (5 mice) (20×).

the glutamate-glutamine cycle.

First, we found that NRG-1/ErbB4 activity is increased in the hippocampus ipsilateral to injection 7 days post-IHKA induced SE while exogenous NRG-1 treatment significantly increases NRG-1/ErbB4 activity in both hippocampi. We observed a layer-specific increase in NRG-1/phospho-ErbB4 immunoreactivity in *CA1* of the ipsilateral hippocampus. NRG-1 immunoreactivity was increased in *s. oriens*, *s. pyramidale* of *CA1*, *s. radiatum*, and *s. lacunosum moleculare* of the ipsilateral hippocampus 7 days post-IHKA induced SE. Phospho-ErbB4 immunoreactivity was also increased in s. pyramidale of CA1 in the ipsilateral hippocampus. ErbB4 activity was markedly increased throughout both hippocampi in NRG-1 treated mice at 7 days post-IHKA induced SE.

The highest levels of ErbB4 activity was observed in *s. pyramidale* of the ipsilateral hippocampus. *S. pyramidale* contains the cell bodies of *CA1* excitatory neurons and many interneurons. Previous studies have shown that ErbB4 in parvalbumin-positive interneurons plays a critical role in regulating epileptogenesis and deletion of ErbB4 in parvalbumin-expressing interneurons promotes kindling-induced epileptogenesis (Tan et al., 2011). NRG-1 signaling through ErbB4 on parvalbumin expressing interneurons has also been shown to modulate expression of EAAC1 (Yu et al., 2015). Interestingly, we did not observe a difference in parvalbumin-positive interneurons in mice treated with 25 μg/kg NRG-1 compared to vehicle, but we did observe an increase in EAAC1 in mice treated with NRG-1 at 7 days post-IHKA induced SE. In NRG-1 treated mice, EAAC1 co-localized with parvalbumin expressing interneurons but a majority of EAAC1 was not co-localized with parvalbumin expressing interneurons suggesting that exogenous NRG-1 treatment is modulating EAAC1 in another type of neuron or glial cell. EAAC1 expression has been shown to be enriched in pyramidal neurons (Gottlieb et al., 2000) and could be upregulated in these excitatory neurons in NRG-1 treated mice at 7 days post-IHKA induced SE.

ErbB4 receptors are highly expressed in neurons but have also been

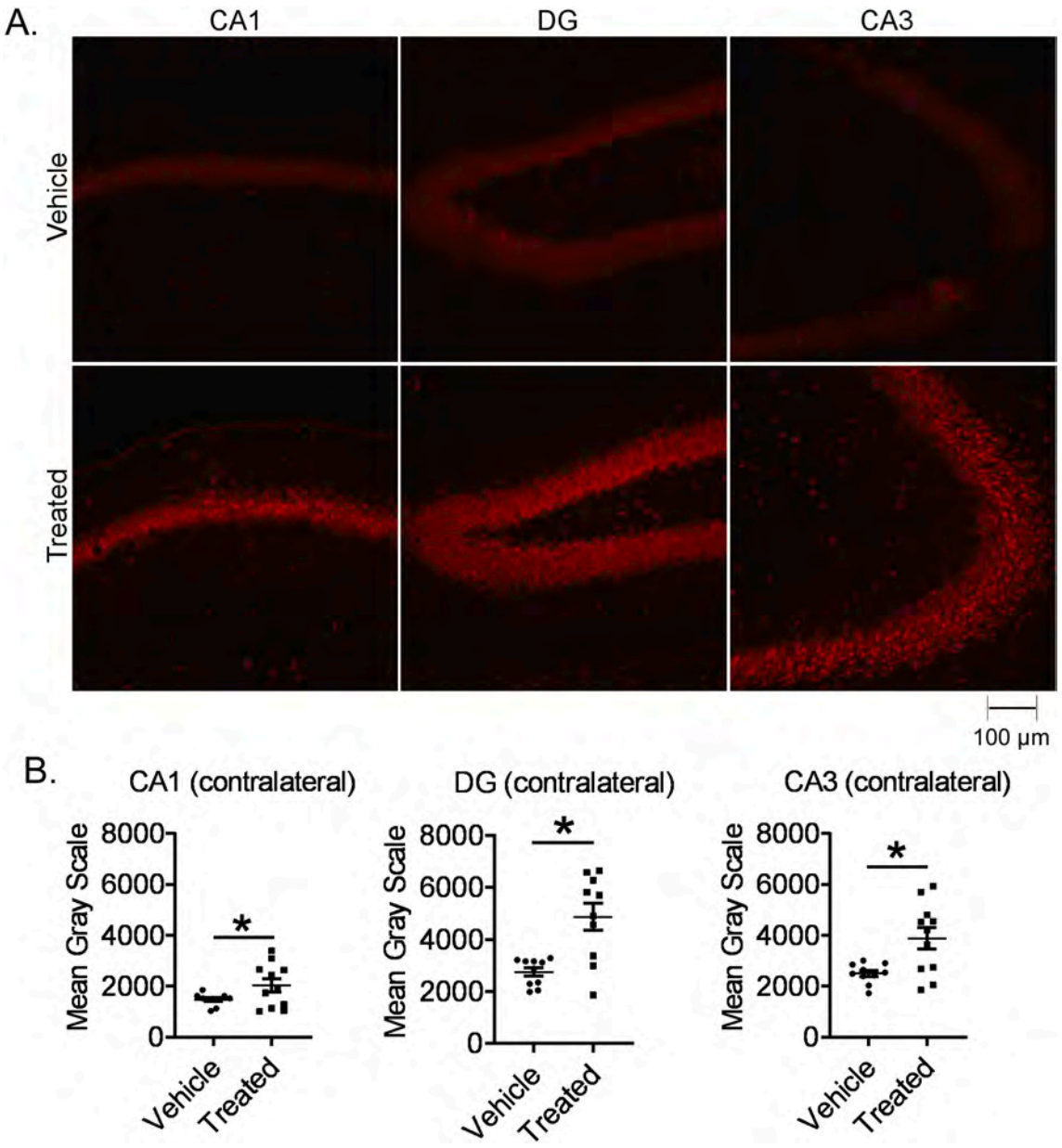

Fig. 17. NeuN immunoreactivity is increased 7 days post-IHKA induced SE in the contralateral hippocampus of NRG-1 treated mice. Coronal section of the contralateral hippocampus 7 days post-IHKA induced SE showing expression and quantitation of NeuN immunoreactivity in CA1, DG, and CA3 of NRG-1 treated mice *vs.* vehicle. Vehicle group; N = 10 sections (5 mice). NRG-1 Treatment group; N = 10 sections (5 mice) (20×).

reported in oligodendrocytes and astrocytes (Roy et al., 2007; Sharif et al., 2009). Reactive astrocytes have been shown to produce NRG-1 which may stimulate their proliferation and support surviving neurons following an insult to the CNS (Tokita et al., 2001). In NRG-1 treated mice, we observed NRG-1 and phospho-ErbB4 co-localization with $GFAP^{+}$ cells (Fig. 18) suggesting that NRG-1/ErbB4 signaling is increased in reactive astrocytes in epileptogenesis. Interestingly, we observed an upregulation of the astrocytic marker GFAP in NRG-1 treated mice compared to controls at 7 days post-IHKA induced SE. These data suggest that NRG-1/ErbB4 signaling in astrocytes is important for their proliferation. We observed an increase in GFAP in the dentate gyrus and *CA3* suggesting this signaling is region specific. Previous studies have reported that astrocytic ErbB4 activation could play a role in the induction of reactive astrogliosis (Chen et al., 2017). Interestingly, we did not observe a difference in astrocytic glutamate transporters, GLT-1 or GLAST, in NRG-1 treated mice suggesting that NRG-1/ErbB4 signaling selectively targets the glutamate transporter EAAC1.

Downstream signaling pathways of ErbB4 tyrosine receptor dimerization have been shown to regulate cell proliferation, survival, and inflammatory responses (Olayioye et al., 2000; Yarden and Sliwkowski, 2001; Mei and Nave, 2014). These data suggest reactive astrocytes could be releasing NRG-1 which is further enhanced with exogenous NRG-1 treatment to support survival in surrounding neurons. Astroglial ErbB signaling has been shown to play a crucial role in the development and maintenance of the CNS through neuron-glia communication. For example, in ErbB1 knockout-mice astrocytes undergo apoptosis decreasing their ability to support neuronal survival which eventually leads to neurodegeneration (Wagner et al., 2006). ErbB4 signaling plays a critical role in several aspects of neuronal development including controlling the onset of astrogenesis and dendrite morphology suggesting dysregulation of this pathway could lead to neuropathology associated with many neurological diseases (Rieff and Corfas, 2006; Sardi et al., 2006).

Glutamine synthetase (GS), an enzyme found primarily in astrocytes,

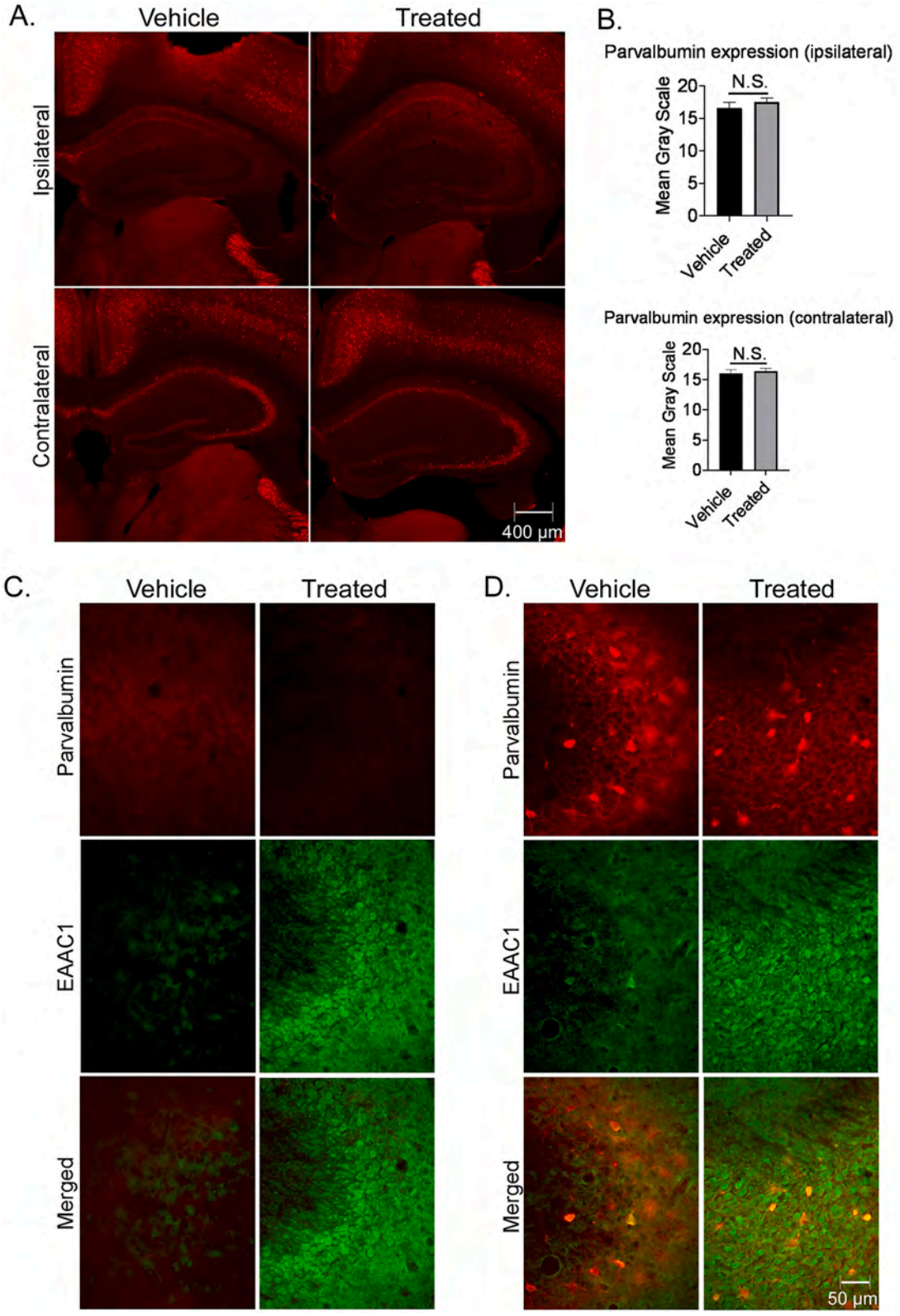

Fig. 18. Hippocampal parvalbumin expression is not changed in mice treated with 25 μg/kg NRG-1 7 days post-IHKA induced SE. A. Parvalbumin (red) expression in the ipsilateral and contralateral hippocampus of NRG-1-treated *vs.* vehicle-treated mice at 7 days post-IHKA induced SE (5×). B. Parvalbumin mean gray scale quantitation of ipsilateral and contralateral hippocampus of NRG-1-treated *vs.* vehicle-treated mice at 7 days post-IHKA induced SE. C. Parvalbumin (red) expression and EAAC1 (green) expression in the ipsilateral and contralateral hippocampus of NRG-1-treated *vs.* vehicle-treated mice at 7 days post-IHKA induced SE (40×). Vehicle group; N = 6 sections (4 mice). NRG-1 Treatment group; N = 10 sections (5 mice). (For interpretation of the references to colour in this figure legend, the reader is referred to the web version of this article.)

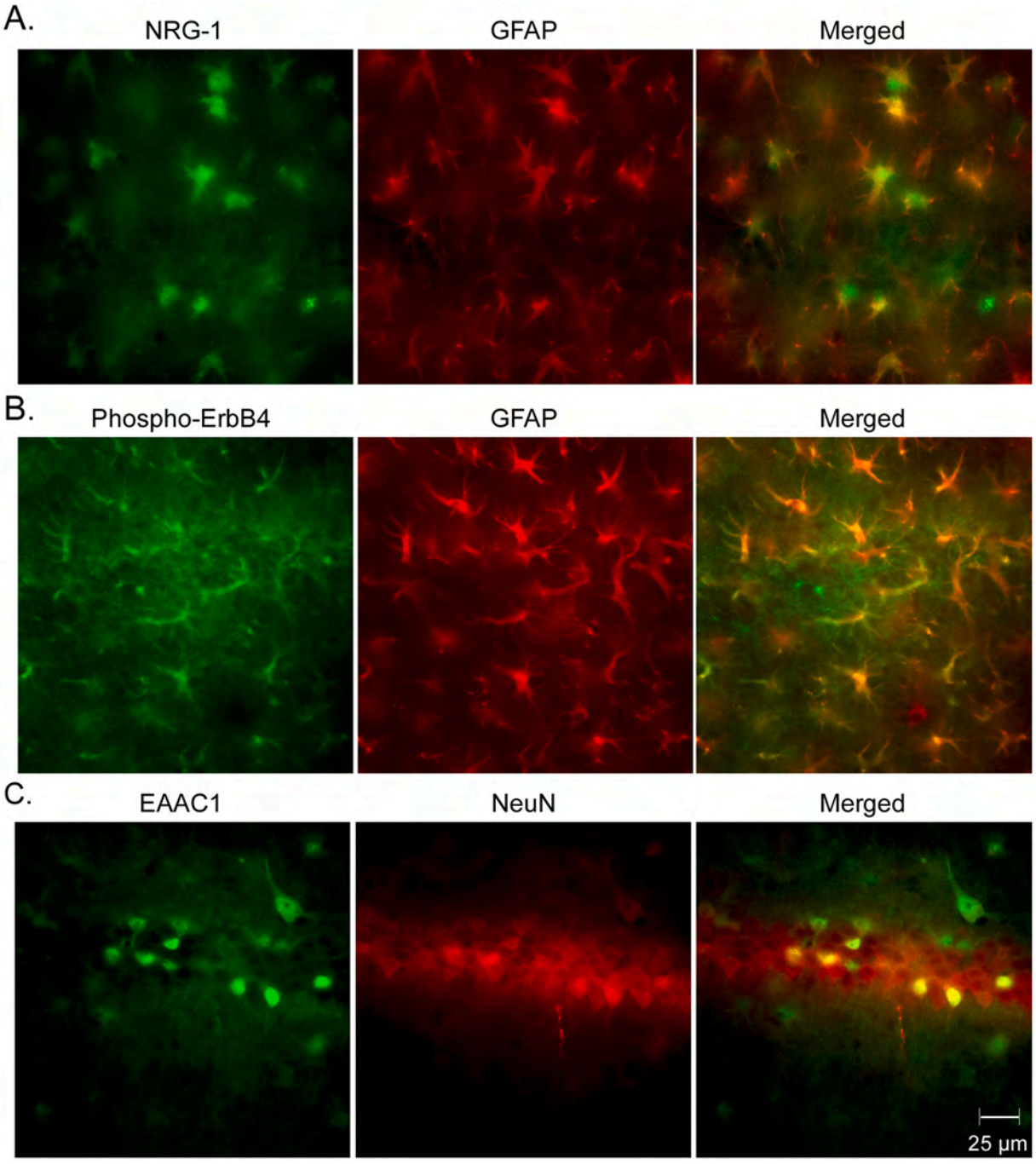

Fig. 19. Expression of NRG-1, Phospho-ErbB4 and EAAC1 in the hippocampus of NRG-1 treated mice 7 days post-IHKA induced SE. A. NRG-1 (green) and GFAP (red) expression in the hippocampus of NRG-1 treated mice. B. Phospho-ErbB4 (green) and GFAP (red) expression in the hippocampus of NRG-1 treated mice. C. EAAC1 (green) and NeuN (red) expression in the hippocampus of NRG-1 treated mice (63×). (For interpretation of the references to colour in this figure legend, the reader is referred to the web version of this article.)

is responsible for the rapid conversion of intracellular glutamate to glutamine and is a prerequisite for efficient glutamate clearance from the extracellular space (Martinez-Hernandez et al., 1977). GS is critical for glutamate metabolism and deficiencies in this enzyme could lead to increased glutamate in the extracellular space and decreased glutamate clearance (Petroff et al., 2002; van der Hel et al., 2005). GS protein levels have been shown to be reduced in the epileptogenic hippocampal formation in patients with MTLE suggesting that GS deficiency could be a contributing factor in the development of epilepsy (Eid et al., 2004). Second, we observed an increase in GS in NRG-1 treated mice compared to controls at 7 days post-IHKA induced SE. Our data suggest that NRG-1/ErbB4 signaling in astrocytes leads to upregulation of GS which could be neuroprotective against glutamate neurotoxicity. Therefore, neuroprotection by NRG-1 could be due to its effect on glutamate-glutamine cycling in restoring glutamate homeostasis. Regulation of extracellular glutamate is crucial for efficient and localized synaptic activity (Danbolt, 2001).

Third, we observed a decrease in Iba^{+} immunoreactivity, a marker for reactive microglia, in the contralateral hippocampus of NRG-1 treated mice compared to vehicle (Supplementary Fig. 3). Neuroinflammation and microglial activation has previously been observed in human epileptic tissue and rodent models of epilepsy (Gershen et al.,

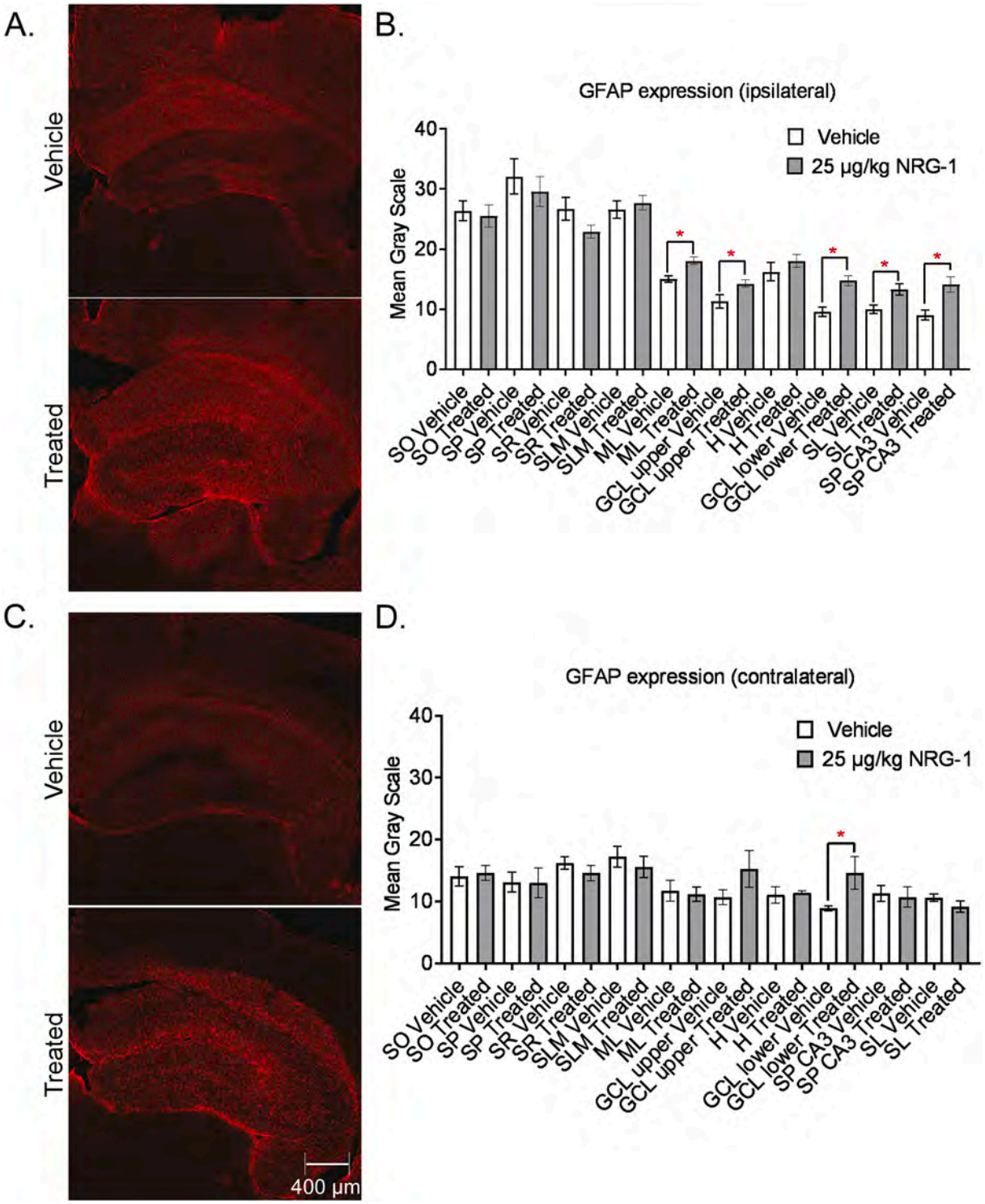

Fig. 20. GFAP expression is increased in the both hippocampi of mice treated with 25 µg/kg NRG-1 7 days post-IHKA induced SE. A. GFAP (red) in the ipsilateral hippocampus of NRG-1-treated *vs.* vehicle-treated mice at 7 days post-IHKA induced SE (5×). B. GFAP mean gray scale quantitation of individual cell layers. C. GFAP (red) in the contralateral hippocampus of NRG-1-treated *vs.* vehicle-treated mice at 7 days post-IHKA induced SE (5×). D. GFAP mean gray scale quantitation of individual cell layers. Vehicle group; N = 10 sections (5 mice). NRG-1 Treatment group; N = 11 sections (6 mice). (For interpretation of the references to colour in this figure legend, the reader is referred to the web version of this article.)

2015; Schartz et al., 2016; Wyatt-Johnson et al., 2017; Morin-Brureau et al., 2018). Previous studies have reported at NRG-1/ErbB4 signaling promotes microglia proliferation and chemotaxis (Calvo et al., 2010) while others have reported that NRG-1's anti-inflammatory effects are associated with differential regulation of NF-kB signaling pathways and suppression of pro-inflammatory gene expression in microglia (Simmons et al., 2016). We observed a decrease in Iba + immunoreactivity suggesting that NRG-1 treatment suppresses pro-inflammatory signaling in these mice. Interestingly, the contralateral hippocampus is also where we observed the majority of differences between NeuN immunoreactivity in all regions investigated; *CA1*, the dentate gyrus and *CA3*. Our data suggest that NRG-1 treatment has anti-inflammatory effects at early

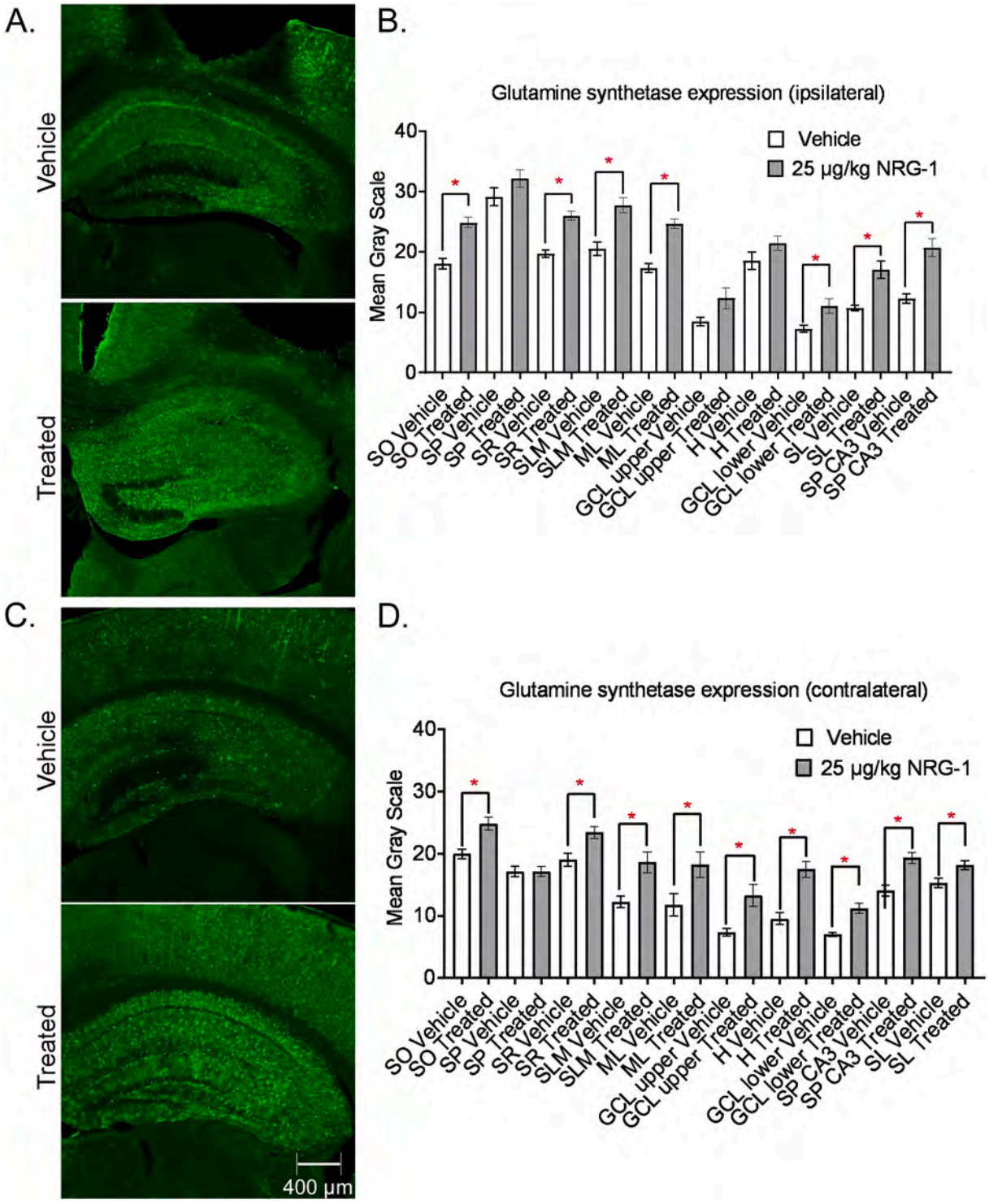

Fig. 21. Glutamine synthetase (GS) expression is increased in the both hippocampi of mice treated with 25 µg/kg NRG-1 7 days post-IHKA induced SE. A. GS (green) in the ipsilateral hippocampus of NRG-1 treated *vs.* vehicle treated mice at 7 days post-IHKA induced SE (5×). B. GS mean gray scale quantitation of individual cell layers. C. GS (green) in the contralateral hippocampus of NRG-1 treated *vs.* vehicle treated mice at 7 days post-IHKA induced SE (5×). D. GS mean gray scale quantitation of individual cell layers. Vehicle group; N = 10 sections (5 mice). NRG-1 Treatment group; N = 12 sections (6 mice). (For interpretation of the references to colour in this figure legend, the reader is referred to the web version of this article.)

time points during the development of epilepsy.

Fourth, we found that EAAC1 immunoreactivity was downregulated at 7 days post-IHKA induced SE and NRG-1 treatment rescued EAAC1 expression in the ipsilateral hippocampus while upregulating EAAC1 expression in hippocampus contralateral to injection. EAAC1 immunoreactivity was significantly decreased in *s. oriens*, *s. pyramidale*, *s. radiatum* and *s. lacunosum moleculare* in the *CA1* region in the ipsilateral hippocampus at 7 days post-IHKA induced SE compared to saline injected control mice. We have previously reported that astrocytic glutamate transporter, GLT-1 is also significantly downregulated one week following IHKA-induced SE which corresponds well with the onset of spontaneous seizures in this model (Peterson and Binder, 2019).

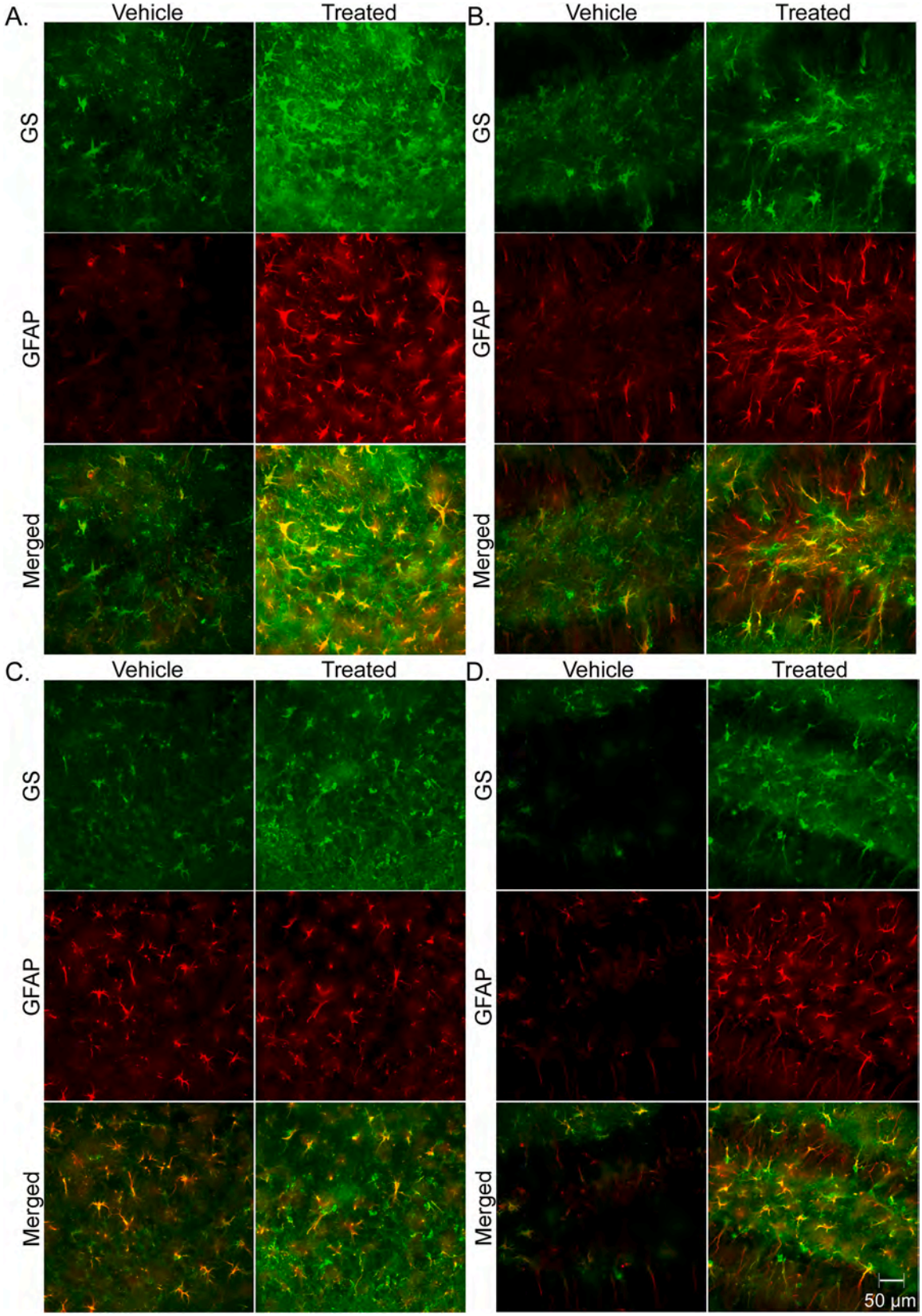

Fig. 22. Glutamine synthetase (GS) and GFAP is increased in the both hippocampi of mice treated with 25 µg/kg NRG-1 7 days post-IHKA induced SE. A. GS (green) and GFAP (red) expression in CA3 region of the ipsilateral hippocampus. B. GS (green) and GFAP (red) expression in DG region of the ipsilateral hippocampus. C. GS (green) and GFAP (red) expression in CA3 region of the contralateral hippocampus. D. GS (green) and GFAP (red) expression in DG region of the contralateral hippocampus (40×). (For interpretation of the references to colour in this figure legend, the reader is referred to the web version of this article.)

EAAC1 is primarily found on dendrites and somata of pyramidal cells and GABAergic neurons (Conti et al., 1998). Administration of antisense oligonucleotides to EAAC1 has been shown to produce facial twitches, freezing behavior and clonic seizures, suggesting EAAC1 could play an important role in regulating glutamate homeostasis in the epileptic brain (Rothstein et al., 1996). EAAC1 knockout mice are more sensitive to ischemia-induced cell death but have also been shown to experience less cell death compared to control animals after pilocarpine-induced seizures suggesting EAAC1 trafficking might be differentially affected in disease (Won et al., 2010; Lane et al., 2014). Interestingly, EAAC1 has also been shown to be elevated in epileptic rats following pilocarpine-induced SE and in patients with epilepsy, suggesting that these transporters could alter neurotransmission in patients with TLE (Mathern et al., 1999; Crino et al., 2002). EAAC1 expression was significantly increased in both hippocampi of NRG-1-treated mice at 7 days post-IHKA induced SE. EAAC1 expression was upregulated in *s. pyramidale* of *CA1* in parallel to the upregulation of phospho-ErbB4 immunoreactivity observed in the ipsilateral hippocampus of NRG-1 treated mice. NRG-1/ErbB4 activation has been shown to upregulate EAAC1 and increase glutamate uptake in cortical neurons, suggesting that EAAC1 may play an important role in synaptic activity and neurotransmission (Yu et al., 2015). In NRG-1-treated mice, EAAC1 expression was increased throughout all layers of the contralateral hippocampus associated with an increase in NeuN immunoreactivity, suggesting a neuroprotective role of NRG-1 *via* EAAC1 upregulation. In order to determine if NRG-1 treated mice have increased glutamate uptake, future studies could examine extracellular glutamate levels in both hippocampi using an enzymatic glutamate biosensor or microdialysis. Functional studies could also be performed using synaptosomal glutamate uptake assays to determine if EAAC1-mediated glutamate uptake is increased in NRG-1 treated mice (Petr et al., 2015). EAAC1 is also a major route for neuronal cysteine uptake which is important for the synthesis of glutathione (GSH). GSH is an antioxidant which protects cells against the accumulation of reactive oxygen species and has been shown to be reduced in patients with epilepsy (Mueller et al., 2001). Mice deficient in EAAC1 have reduced neuronal glutathione and increased susceptibility to oxidant injury (Aoyama et al., 2006). NRG-1 has been shown to promote glutathione-dependent vitamin B_{12} metabolism by increasing cysteine uptake (Zhang et al., 2016). Future studies could determine whether NRG-1/ErbB4 activity is important for EAAC1-dependent glutathione synthesis in epileptogenesis and whether it is responsible for the neuroprotective effects observed with NRG-1 treatment. Recently, a novel probe was synthesized to visualize endogenous and exogenous GSH *via* fluorescence imaging. This probe could be used to determine if GSH levels are increased in EAAC1 expressing neurons of NRG-1 treated mice (Niu et al., 2020).

Fifth, we found that NeuN-positive neurons are reduced 7 days post-IHKA induced SE while NRG-1 treatment rescued NeuN immunoreactivity in both hippocampi. Widespread neuronal cell loss associated with TLE occurs in *CA1*, the dentate gyrus and *CA3* in the hippocampus (Scharfman and Gray, 2007). In this study, NeuN immunoreactivity was significantly reduced in *CA1*, the dentate gyrus, and *CA3* in both hippocampi of epileptic mice at 7 days post-IHKA compared to saline-injected control mice. SE-induced neuronal death has been reported in many animal models of epilepsy and in patients (Sankar et al., 1998; Fujikawa et al., 2000) and distant neuronal damage has previously been reported following unilateral kainic acid injections (Magloczky and Freund, 1993). Interestingly, NRG-1 treated mice had significantly higher NeuN immunoreactivity in *CA1* and *CA3* of the contralateral hippocampus and the dentate gyrus of both hippocampi compared to vehicle. Likewise, NRG-1 treatment has been shown to rescue NeuN immunoreactivity in a mouse model of focal ischemic stroke and has been shown to suppress seizure-induced mossy fiber sprouting (Tan et al., 2011; Noll et al., 2019). To our knowledge, this is the first study to report neuroprotective effects of NRG-1 treatment in both hippocampi following unilateral kainic acid injection. Interestingly, despite a majority of seizures initiating in the ipsilateral hippocampus, neuronal loss can be observed in both hippocampi (Riban et al., 2002). These data suggest that NRG-1 treatment is neuroprotective at early time points in epilepsy potentially through NRG/ErbB4 dependent upregulation of glutamate transporter EAAC1. Future studies could examine whether NRG-1 treatment is neuroprotective in EAAC1 knockout mice challenged with kainic acid to determine whether EAAC1 is responsible for the increase in NeuN immunoreactivity observed in NRG-1 treated mice.

Overall, in this study we demonstrated that NRG-1 treatment is neuroprotective in epileptogenesis likely through restoration of glutamate homeostasis. Previous studies have shown that extracellular glutamate levels are increased prior to seizure onset in patients with TLE and remain elevated shortly after (During and Spencer, 1993). Recent data also suggest that basal levels of extracellular glutamate are elevated in patients with refractory epilepsy (Cavus et al., 2016). These studies imply that dysregulation of glutamate homeostasis could be contributing to epilepsies that are refractory to currently available AEDs. Upregulation of glutamine synthetase and glutamate transporter EAAC1 by NRG-1 could reduce extracellular glutamate levels and therefore potentially abrogate recurrent seizures and thus serve as an alternative therapeutic option for refractory TLE. In a phase II clinical trial in patients with heart failure, NRG-1 treatment improved cardiac function and the effective dose was safe and well tolerated (Gao et al., 2010); these data suggest that NRG-1 could be tested safely for therapeutic efficacy in patients with refractory epilepsies.

5. Conclusion

In summary, we report the first evaluation of NRG-1/ErbB4 dependent selective upregulation of glutamate transporter EAAC1 and bihemispheric neuroprotection by exogeneous NRG-1 in a mouse model of temporal lobe epilepsy. Our findings provide evidence that ErbB4/NRG-1 signaling can be therapeutically targeted and is neuroprotective by restoring glutamate homeostasis through upregulation of glutamine synthetase and glutamate transporter EAAC1 following IHKA induced SE.

Supplementary data to this article can be found online at https://doi.org/10.1016/j.nbd.2021.105545.

Author contributions

ARP, BDF, and DKB conceived of the project. ARP and DKB designed experiments. ARP and TAG performed experiments and analyzed the results. ARP and DKB co-wrote the manuscript. All co-authors edited and approved the final version of the manuscript.

Funding

This research did not receive any specific grant from funding agencies in the public, commercial, or not-for-profit sectors.

Declaration of Competing Interest

The authors declare no competing interests.

Acknowledgements

The authors would like to thank Carrie Jonak for breeding the mice used for this study and Jessica Noll for providing the NRG-1 used for preliminary studies.

References

Aoyama, K., Suh, S.W., Hamby, A.M., Liu, J., Chan, W.Y., Chen, Y., Swanson, R.A., 2006. Neuronal glutathione deficiency and age-dependent neurodegeneration in the EAAC1 deficient mouse. Nat. Neurosci. 9 (1), 119–126.

Beck, H. Y. Yaari (2012). Antiepileptogenesis, plasticity of AED targets, drug resistance, and targeting the immature brain. Jasper's Basic Mechanisms of the Epilepsies. J. L. Noebels, M. Avoli et al. Bethesda (MD).
Brodie, M.J., Besag, F., Ettinger, A.B., Mula, M., Gobbi, G., Comai, S., Aldenkamp, A.P., Steinhoff, B.J., 2016. Epilepsy, antiepileptic drugs, and aggression: an evidence-based review. Pharmacol. Rev. 68 (3), 563–602.
Calvo, M., Zhu, N., Tsantoulas, C., Ma, Z., Grist, J., Loeb, J.A., Bennett, D.L., 2010. Neuregulin-ErbB signaling promotes microglial proliferation and chemotaxis contributing to microgliosis and pain after peripheral nerve injury. J. Neurosci. 30 (15), 5437–5450.
Cannella, B., Pitt, D., Marchionni, M., Raine, C.S., 1999. Neuregulin and erbB receptor expression in normal and diseased human white matter. J. Neuroimmunol. 100 (1–2), 233–242.
Cavus, I., Romanyshyn, J.C., Kennard, J.T., Farooque, P., Williamson, A., Eid, T., Spencer, S.S., Duckrow, R., Dziura, J., Spencer, D.D., 2016. Elevated basal glutamate and unchanged glutamine and GABA in refractory epilepsy: microdialysis study of 79 patients at the Yale epilepsy surgery program. Ann. Neurol. 80 (1), 35–45.
Cespedes, J.C., Liu, M., Harbuzariu, A., Nti, A., Onyekaba, J., Cespedes, H.W., Bharti, P. K., Solomon, W., Anyaoha, P., Krishna, S., Adjei, A., Botchway, F., Ford, B., Stiles, J. K., 2018. Neuregulin in health and disease. Int. J. Brain Disord. Treat. 4 (1).
Chen, J., He, W., Hu, X., Shen, Y., Cao, J., Wei, Z., Luan, Y., He, L., Jiang, F., Tao, Y., 2017. A role for ErbB signaling in the induction of reactive astrogliosis. Cell Discov. 3, 17044.
Conti, F., DeBiasi, S., Minelli, A., Rothstein, J.D., Melone, M., 1998. EAAC1, a high-affinity glutamate tranporter, is localized to astrocytes and gabaergic neurons besides pyramidal cells in the rat cerebral cortex. Cereb. Cortex 8 (2), 108–116.
Crino, P.B., Jin, H., Shumate, M.D., Robinson, M.B., Coulter, D.A., Brooks-Kayal, A.R., 2002. Increased expression of the neuronal glutamate transporter (EAAT3/EAAC1) in hippocampal and neocortical epilepsy. Epilepsia 43 (3), 211–218.
Dalic, L., Cook, M.J., 2016. Managing drug-resistant epilepsy: challenges and solutions. Neuropsychiatr. Dis. Treat. 12, 2605–2616.
Danbolt, N.C., 2001. Glutamate uptake. Prog. Neurobiol. 65 (1), 1–105.
Deng, W., Luo, F., Li, B.M., Mei, L., 2019. NRG1-ErbB4 signaling promotes functional recovery in a murine model of traumatic brain injury via regulation of GABA release. Exp. Brain Res. 237 (12), 3351–3362.
During, M.J., Spencer, D.D., 1993. Extracellular hippocampal glutamate and spontaneous seizure in the conscious human brain. Lancet 341, 1607–1610.
Eid, T., Thomas, M.J., Spencer, D.D., Runden-Pran, E., Lai, J.C., Malthankar, G.V., Kim, J. H., Danbolt, N.C., Ottersen, O.P., de Lanerolle, N.C., 2004. Loss of glutamine synthetase in the human epileptogenic hippocampus: possible mechanism for raised extracellular glutamate in mesial temporal lobe epilepsy. Lancet 363 (9402), 28–37.
Eid, T., Tu, N., Lee, T.S., Lai, J.C., 2013. Regulation of astrocyte glutamine synthetase in epilepsy. Neurochem. Int. 63 (7), 670–681.
Erlich, S., Shohami, E., Pinkas-Kramarski, R., 2000. Closed head injury induces up-regulation of ErbB-4 receptor at the site of injury. Mol. Cell. Neurosci. 16 (5), 597–608.
Fisher, R.S., Acevedo, C., Arzimanoglou, A., Bogacz, A., Cross, J.H., Elger, C.E., Engel Jr., J., Forsgren, L., French, J.A., Glynn, M., Hesdorffer, D.C., Lee, B.I., Mathern, G.W., Moshe, S.L., Perucca, E., Scheffer, I.E., Tomson, T., Watanabe, M., Wiebe, S., 2014. ILAE official report: a practical clinical definition of epilepsy. Epilepsia 55 (4), 475–482.
Fujikawa, D.G., Itabashi, H.H., Wu, A., Shinmei, S.S., 2000. Status epilepticus-induced neuronal loss in humans without systemic complications or epilepsy. Epilepsia 41 (8), 981–991.
Gao, R., et al., 2010. A phase II, randomized, double-blind, multicenter, based on standard therapy, placebo-controlled study of the efficacy and safety of recombinant human neuregulin-1 in patients with chronic heart failure. J. Am. Coll. Cardiol. 55, 1907–1914.
Gershen, L.D., Zanotti-Fregonara, P., Dustin, I.H., Liow, J.S., Hirvonen, J., Kreisl, W.C., Jenko, K.J., Inati, S.K., Fujita, M., Morse, C.L., Brouwer, C., Hong, J.S., Pike, V.W., Zoghbi, S.S., Innis, R.B., Theodore, W.H., 2015. Neuroinflammation in temporal lobe epilepsy measured using positron emission tomographic imaging of translocator protein. JAMA Neurol. 72 (8), 882–888.
Gottlieb, M., Domercq, M., Matute, C., 2000. Altered expression of the glutamate transporter EAAC1 in neurons and immature oligodendrocytes after transient forebrain ischemia. J. Cereb. Blood Flow Metab. 20 (4), 678–687.
van der Hel, W.S., Notenboom, R.G., Bos, I.W., van Rijen, P.C., van Veelen, C.W., de Graan, P.N., 2005. Reduced glutamine synthetase in hippocampal areas with neuron loss in temporal lobe epilepsy. Neurology 64 (2), 326–333.
Hubbard, J.A., Szu, J.I., Yonan, J.M., Binder, D.K., 2016. Regulation of astrocyte glutamate transporter-1 (GLT1) and aquaporin-4 (AQP4) expression in a model of epilepsy. Exp. Neurol. 283 (Pt A), 85–96.
Lane, M.C., Jackson, J.G., Krizman, E.N., Rothstein, J.D., Porter, B.E., Robinson, M.B., 2014. Genetic deletion of the neuronal glutamate transporter, EAAC1, results in decreased neuronal death after pilocarpine-induced status epilepticus. Neurochem. Int. 73, 152–158.
Lee, S.K., 2014. Old versus new: why do we need new antiepileptic drugs? J. Epilepsy Res. 4 (2), 39–44.
Lee, D.J., Hsu, M.S., Seldin, M.M., Arellano, J.L., Binder, D.K., 2012. Decreased expression of the glial water channel aquaporin-4 in the intrahippocampal kainic acid model of epileptogenesis. Exp. Neurol. 235 (1), 246–255.
Liu, M., Solomon, W., Cespedes, J.C., Wilson, N.O., Ford, B., Stiles, J.K., 2018. Neuregulin-1 attenuates experimental cerebral malaria (ECM) pathogenesis by regulating ErbB4/AKT/STAT3 signaling. J. Neuroinflammation 15 (1), 104.
Magloczky, Z., Freund, T.F., 1993. Selective neuronal death in the contralateral hippocampus following unilateral kainate injections into the CA3 subfield. Neuroscience 56 (2), 317–335.
Mahmoud, S., Gharagozloo, M., Simard, C., Gris, D., 2019. Astrocytes maintain glutamate homeostasis in the CNS by controlling the balance between glutamate uptake and release. Cells 8 (2).
Martinez-Hernandez, A., Bell, K.P., Norenberg, M.D., 1977. Glutamine synthetase: glial localization in brain. Science 195 (4284), 1356–1358.
Mathern, G.W., Mendoza, D., Lozada, A., Pretorius, J.K., Dehnes, Y., Danbolt, N.C., Nelson, N., Leite, J.P., Chimelli, L., Born, D.E., Sakamoto, A.C., Assirati, J.A., Fried, I., Peacock, W.J., Ojemann, G.A., Adelson, P.D., 1999. Hippocampal GABA and glutamate transporter immunoreactivity in patients with temporal lobe epilepsy. Neurology 52 (3), 453–472.
Mei, L., Nave, K.A., 2014. Neuregulin-ERBB signaling in the nervous system and neuropsychiatric diseases. Neuron 83 (1), 27–49.
Morin-Brureau, M., Milior, G., Royer, J., Chali, F., Le Duigou, C., Savary, E., Blugeon, C., Jourdren, L., Akbar, D., Dupont, S., Navarro, V., Baulac, M., Bielle, F., Mathon, B., Clemenceau, S., Miles, R., 2018. Microglial phenotypes in the human epileptic temporal lobe. Brain 141 (12), 3343–3360.
Mueller, S.G., Trabesinger, A.H., Boesiger, P., Wieser, H.G., 2001. Brain glutathione levels in patients with epilepsy measured by in vivo (1)H-MRS. Neurology 57 (8), 1422–1427.
Niu, T., Yin, G., Yu, T., Gan, Y., Zhang, C., Chen, J., Wu, W., Chen, H., Li, H., Yin, P., 2020. A novel fluorescent probe for detection of glutathione dynamics during ROS-induced redox imbalance. Anal. Chim. Acta 1115, 52–60.
Noll, J.M., Li, Y., Distel, T.J., Ford, G.D., Ford, B.D., 2019. Neuroprotection by exogenous and endogenous Neuregulin-1 in mouse models of focal ischemic stroke. J. Mol. Neurosci. 69 (2), 333–342.
Olayioye, M.A., Neve, R.M., Lane, H.A., Hynes, N.E., 2000. The ErbB signaling network: receptor heterodimerization in development and cancer. EMBO J. 19 (13), 3159–3167.
Parker, M.W., Chen, Y., Hallenbeck, J.M., Ford, B.D., 2002. Neuregulin expression after focal stroke in the rat. Neurosci. Lett. 334 (3), 169–172.
Peterson, A.R., Binder, D.K., 2019. Regulation of Synaptosomal GLT-1 and GLAST during Epileptogenesis. Neuroscience 411, 185–201.
Peterson, A.R., Garcia, T.A., Cullion, K., Tiwari-Woodruff, S.K., Pedapati, E.V., Binder, D. K., 2021. Targeted overexpression of glutamate transporter-1 reduces seizures and attenuates pathological changes in a mouse model of epilepsy. Neurobiol. Dis. 157, 105443.
Petr, G.T., Sun, Y., Frederick, N.M., Zhou, Y., Dhamne, S.C., Hameed, M.Q., Miranda, C., Bedoya, E.A., Fischer, K.D., Armsen, W., Wang, J., Danbolt, N.C., Rotenberg, A., Aoki, C.J., Rosenberg, P.A., 2015. Conditional deletion of the glutamate transporter GLT-1 reveals that astrocytic GLT-1 protects against fatal epilepsy while neuronal GLT-1 contributes significantly to glutamate uptake into synaptosomes. J. Neurosci. 35 (13), 5187–5201.
Petroff, O.A., Errante, L.D., Rothman, D.L., Kim, J.H., Spencer, D.D., 2002. Glutamate-glutamine cycling in the epileptic human hippocampus. Epilepsia 43 (7), 703–710.
Proper, E.A., Hoogland, G., Kappen, S.M., Jansen, G.H., Rensen, M.G., Schrama, L.H., van Veelen, C.W., van Rijen, P.C., van Nieuwenhuizen, O., Gispen, W.H., de Graan, P.N., 2002. Distribution of glutamate transporters in the hippocampus of patients with pharmaco-resistant temporal lobe epilepsy. Brain 125 (Pt 1), 32–43.
Racine, R.J., 1972. Modification of seizure activity by electrical stimulation. II. Motor seizure. Electroencephalogr. Clin. Neurophysiol. 32 (3), 281–294.
Ramandi, D., Elahdadi Salmani, M., Moghimi, A., Lashkarbolouki, T., Fereidoni, M., 2021. Pharmacological upregulation of GLT-1 alleviates the cognitive impairments in the animal model of temporal lobe epilepsy. PLoS One 16 (1), e0246068.
Riban, V., Bouilleret, V., Pham-Le, B.T., Fritschy, J.M., Marescaux, C., Depaulis, A., 2002. Evolution of hippocampal epileptic activity during the development of hippocampal sclerosis in a mouse model of temporal lobe epilepsy. Neuroscience 112 (1), 101–111.
Rieff, H.I., Corfas, G., 2006. ErbB receptor signalling regulates dendrite formation in mouse cerebellar granule cells in vivo. Eur. J. Neurosci. 23 (8), 2225–2229.
Rothstein, J.D., Dykes-Hoberg, M., Pardo, C.A., Bristol, L.A., Jin, L., Kuncl, R.W., Kanai, Y., Hediger, M.A., Wang, Y., Schielke, J.P., Welty, D.F., 1996. Knockout of glutamate transporters reveals a major role for astroglial transport in excitotoxicity and clearance of glutamate. Neuron 16 (3), 675–686.
Roy, K., Murtie, J.C., El-Khodor, B.F., Edgar, N., Sardi, S.P., Hooks, B.M., Benoit-Marand, M., Chen, C., Moore, H., O'Donnell, P., Brunner, D., Corfas, G., 2007. Loss of erbB signaling in oligodendrocytes alters myelin and dopaminergic function, a potential mechanism for neuropsychiatric disorders. Proc. Natl. Acad. Sci. U. S. A. 104 (19), 8131–8136.
Sankar, R., Shin, D.H., Liu, H., Mazarati, A., Pereira de Vasconcelos, A., Wasterlain, C.G., 1998. Patterns of status epilepticus-induced neuronal injury during development and long-term consequences. J. Neurosci. 18 (20), 8382–8393.
Sardi, S.P., Murtie, J., Koirala, S., Patten, B.A., Corfas, G., 2006. Presenilin-dependent ErbB4 nuclear signaling regulates the timing of astrogenesis in the developing brain. Cell 127 (1), 185–197.
Scharfman, H.E., Gray, W.P., 2007. Relevance of seizure-induced neurogenesis in animal models of epilepsy to the etiology of temporal lobe epilepsy. Epilepsia 48 (Suppl. 2), 33–41.
Schartz, N.D., Herr, S.A., Madsen, L., Butts, S.J., Torres, C., Mendez, L.B., Brewster, A.L., 2016. Spatiotemporal profile of Map2 and microglial changes in the hippocampal CA1 region following pilocarpine-induced status epilepticus. Sci. Rep. 6, 24988.
Sharif, A., Duhem-Tonnelle, V., Allet, C., Baroncini, M., Loyens, A., Kerr-Conte, J., Collier, F., Blond, S., Ojeda, S.R., Junier, M.P., Prevot, V., 2009. Differential erbB

signaling in astrocytes from the cerebral cortex and the hypothalamus of the human brain. Glia 57 (4), 362–379.
Shin, E.J., Ko, K.H., Kim, W.K., Chae, J.S., Yen, T.P., Kim, H.J., Wie, M.B., Kim, H.C., 2008. Role of glutathione peroxidase in the ontogeny of hippocampal oxidative stress and kainate seizure sensitivity in the genetically epilepsy-prone rats. Neurochem. Int. 52 (6), 1134–1147.
Simmons, L.J., Surles-Zeigler, M.C., Li, Y., Ford, G.D., Newman, G.D., Ford, B.D., 2016. Regulation of inflammatory responses by neuregulin-1 in brain ischemia and microglial cells in vitro involves the NF-kappa B pathway. J. Neuroinflammation 13 (1), 237.
Singh, A., Trevick, S., 2016. The epidemiology of global epilepsy. Neurol. Clin. 34 (4), 837–847.
Tan, G.H., Liu, Y.Y., Hu, X.L., Yin, D.M., Mei, L., Xiong, Z.Q., 2011. Neuregulin 1 represses limbic epileptogenesis through ErbB4 in parvalbumin-expressing interneurons. Nat. Neurosci. 15 (2), 258–266.
Tokita, Y., Keino, H., Matsui, F., Aono, S., Ishiguro, H., Higashiyama, S., Oohira, A., 2001. Regulation of neuregulin expression in the injured rat brain and cultured astrocytes. J. Neurosci. 21 (4), 1257–1264.
Wagner, B., Natarajan, A., Grunaug, S., Kroismayr, R., Wagner, E.F., Sibilia, M., 2006. Neuronal survival depends on EGFR signaling in cortical but not midbrain astrocytes. EMBO J. 25 (4), 752–762.
Won, S.J., Yoo, B.H., Brennan, A.M., Shin, B.S., Kauppinen, T.M., Berman, A.E., Swanson, R.A., Suh, S.W., 2010. EAAC1 gene deletion alters zinc homeostasis and exacerbates neuronal injury after transient cerebral ischemia. J. Neurosci. 30 (46), 15409–15418.
Wyatt-Johnson, S.K., Herr, S.A., Brewster, A.L., 2017. Status epilepticus triggers time-dependent alterations in microglia abundance and morphological phenotypes in the Hippocampus. Front. Neurol. 8, 700.
Yarden, Y., Sliwkowski, M.X., 2001. Untangling the ErbB signalling network. Nat. Rev. Mol. Cell Biol. 2 (2), 127–137.
Yu, H.N., Park, W.K., Nam, K.H., Song, D.Y., Kim, H.S., Baik, T.K., Woo, R.S., 2015. Neuregulin 1 controls glutamate uptake by up-regulating excitatory amino acid carrier 1 (EAAC1). J. Biol. Chem. 290 (33), 20233–20244.
Zhang, Y., Hodgson, N., Trivedi, M., Deth, R., 2016. Neuregulin 1 promotes glutathione-dependent neuronal cobalamin metabolism by stimulating cysteine uptake. Oxidative Med. Cell. Longev. 2016, 3849087.